Temperature and $-\Delta G^\circ$ Dependence of the Electron Transfer from $BPh^{\cdot -}$ to Q_A in Reaction Center Protein from *Rhodobacter sphaeroides* with Different Quinones as Q_A

M. R. Gunner† and P. Leslie Dutton*

Contribution from the Department of Biochemistry and Biophysics, University of Pennsylvania, Philadelphia, Pennsylvania 19104. *Received July 14, 1988*

Abstract: The rate of electron transfer from $BPh^{\cdot -}$ to Q_A (k_1) was determined at 14, 35, 113, and 298 K in reaction center protein from *Rhodobacter sphaeroides* R-26 in which the native Q_A, UQ_{10}, was removed and activity reconstituted with 22 other quinones. The majority of these had in situ midpoints lower than that of UQ_{10}, diminishing the $-\Delta G^\circ$ for Q_A reduction. The electron-transfer rate was determined from measurement of the quantum yield of $(BChl)_2^{\cdot +}Q_A^{\cdot -}$ (Φ_Q). At 295 K, Φ_Q was obtained from excitation-flash saturation measurements, monitoring $(BChl)_2^{\cdot +}Q_A^{\cdot -}$ formation optically. Between 14 and 113 K, Φ_Q was determined from the amount of $(BChl)_2^{\cdot +}Q_A^{\cdot -}$, measured by EPR, produced by excitation with a subsaturating flash. When the $-\Delta G^\circ$ for the reduction of Q_A by $BPh^{\cdot -}$ was diminished by as much as 150 meV, relative to that found in the native protein, Φ_Q remained ≥ 0.9. However, as the exothermicity was decreased further, Φ_Q diminished steeply. Thus, much of the 650 meV reaction $-\Delta G^\circ$ found in the native RC is required to maintain a near-unity quantum yield. Calculation of the rate of electron transfer from $BPh^{\cdot -}$ to Q_A shows the reaction slows with decreasing exothermicity. However, over the range of $-\Delta G^\circ$ studied, the rate changed little as the system was cooled from 295 to 14 K. These results were analyzed with the model of electron transfer as a nonadiabatic, multiphoton, nonradiative decay process. The persistence of electron transfer at low temperatures over a range of $-\Delta G^\circ$ demonstrates the importance of nuclear tunneling in electron transfer in the photosynthetic reaction center protein. Therefore, the motions of the nuclei as well as electrons must be treated quantum mechanically in the analysis. The $-\Delta G^\circ$ dependence of the rate is consistent with the total reorganization energy being 600 $\pm$ 100 meV for vibrations of frequency ≤ 800 cm^{-1} ($\hbar\omega \leq 100$ meV). The slowing of the rate as the $-\Delta G^\circ$ is diminished, in the absence of significant temperature dependence, suggests that vibrations of $\hbar\omega \approx 15$ meV (120 cm^{-1}) are coupled to the electron transfer and that the reorganization energy of vibrations with $\hbar\omega$ smaller than ≈ 1 meV (8 cm^{-1}) is less than 300 meV. In addition, the results of a similar study of the electron transfer from $Q_A^{\cdot -}$ to $(BChl)_2^{\cdot +}$ (Gunner et al. *J. Phys. Chem.* **1986**, *90*, 3783-3795) are reanalyzed, permitting comparison of the electron-transfer parameters for the two reactions.

The reaction center protein (RC) of purple bacteria provides a unique system for studying the requirements for high-efficiency electron transfer in proteins. When light energy is absorbed by this transmembrane protein, a series of electron-transfer reactions is initiated, resulting in a reduced, low-potential component on one side of the membrane, an oxidized, high-potential component on the other side, and an electric potential difference across the cell membrane.[1-4] The RC has been purified from a variety of bacteria, and it is well established that the in vitro rates of the intraprotein electron-transfer reactions and the yields of the various charge-separated intermediates are essentially the same as those in vivo.[5] In addition, structures of the protein from *Rhodopseudomonas viridis*[6,7] and *Rhodobacter sphaeroides*[8,9] are becoming available at atomic resolution, permitting sophisticated analysis of the relationship between the protein's structure and its function.[10,11]

Studies of the electron-transfer reactions have focused on the RC isolated from *Rb. sphaeroides* strain R-26. Figure 1 summarizes the pathways, rates, and temperature dependence of the reactions in this protein (see ref 1-4 for recent reviews). Electron transfer occurs between tightly bound redox sites, which are held by the surrounding protein in a well-defined orientation and separation.[6-9] The reaction sequence is triggered by the absorption of a photon by a dimer of bacteriochlorophyll [$(BChl)_2$], yielding the excited singlet state [$(BChl)_2$*]. Forward, charge-separating electron transfer consists of $(BChl)_2$* reducing a bacteriopheophytin (BPh), which in turn reduces a ubiquinone-10 (Q_A). In isolated RC, as prepared for the work presented here, the final product is $(BChl)_2^{\cdot +}Q_A^{\cdot -}$. Figure 1 also describes the charge-recombining electron transfers that compete with the forward reactions and so return the protein to the ground state from $(BChl)_2$*, $(BChl)_2^{\cdot +}BPh^{\cdot -}$, or $(BChl)_2^{\cdot +}Q_A^{\cdot -}$.

Each of the intra-RC electron transfers has a characteristic driving force (from 0.2 to 1.2 eV), distance (7-25 Å edge to edge), and reaction rate (varying by 10^9). Thus, several distinct reactions can be studied in this one protein. These reactions occur even at cryogenic temperatures, which has allowed extensive analysis of their temperature dependence.[1,12,14,20-24] In addition, the $-\Delta G^\circ$ of intra-RC reactions involving Q_A can be altered by replacing the native Q_A, ubiquinone-10 (UQ_{10}), with quinones of different in situ midpoint potentials.[15,21,25-28] These Q_A-replaced RCs have

(1) Parson, W. W.; Ke, B. In *Photosynthesis: Energy Conversion in Plants and Bacteria*; Govindjee, Ed.; Academic Press: New York, 1982; pp 331-385.
(2) Okamura, M. Y.; Feher, G.; Nelson, N. In *Photosynthesis: Energy Conversion in Plants and Bacteria*; Govindjee, Ed.; Academic Press: New York, 1982; pp 195-272.
(3) Dutton, P. L. In *Photosynthesis III: Photosynthetic Membranes and Light Harvesting Systems*; Staehelin, L. A.; Arntzen, C. J., Eds.; Springer-Verlag: Berlin; pp 197-237.
(4) Budil, D. E.; Gast, P.; Chang, C.-H.; Schiffer, M.; Norris, J. R. *Annu. Rev. Phys. Chem.* **1987**, *38*, 561-583.
(5) Clayton, R. K.; Sistrom, W. R. *The Photosynthetic Bacteria*; Plenum: New York, 1978.
(6) Deisenhofer, J.; Epp, O.; Miki, R.; Michel, H. *Nature* **1985**, *318*, 618-624.
(7) Michel, H.; Epp, O.; Deisenhofer, J. *EMBO J.* **1986**, *5*, 2445-2451.
(8) Chang, C. H.; Tiede, D.; Tang, J.; Smith, U.; Norris, J.; Schiffer, M. *FEBS Lett.* **1986**, *205*, 82-86.
(9) Allen, J. P.; Feher, G.; Yeates, T. O.; Komiya, H.; Rees, D. C. *Proc. Natl. Acad. Sci. U.S.A.* **1987**, *84*, 5730-5734.
(10) Michel-Beyerle, M. E., Ed. *Antennas and Reaction Centers of Photosynthetic Bacteria*; Springer-Verlag: Berlin, 1985.
(11) Austin, R.; Buhks, E.; Chance, B.; DeVault, D.; Dutton, P. L.; Frauenfelder, H.; Gol'danskii, V. I., Eds. *Protein Structure: Molecular and Electronic Reactivity*; Springer-Verlag: New York, 1987.
(12) Woodbury, N. W. T.; Becker, N.; Kirmaier, C.; Holten, D. *Biochemistry* **1985**, *24*, 7516-7521.
(13) Martin, J. L.; Breton, J.; Hoff, A. J.; Migus, A.; Antonetti, A. *Proc. Natl. Acad. Sci. U.S.A.* **1986**, *83*, 957-967.
(14) Kirmaier, C.; Holten, D.; Parson, W. W. *Biochim. Biophys. Acta* **1985**, *810*, 33-48.
(15) Woodbury, N. W. T.; Parson, W. W.; Gunner, M. R.; Prince, R. C.; Dutton, P. L. *Biochim. Biophys. Acta* **1986**, *851*, 6-22.
(16) Zankel, K. L.; Reed, D. W.; Clayton, R. K. *Proc. Natl. Acad. Sci. U.S.A.* **1968**, *61*, 1243-1249.
(17) Chidsey, C. E. D.; Kirmaier, C.; Holten, D.; Boxer, S. G. *Biochim. Biophys. Acta* **1984**, *766*, 424-437.
(18) Budil, D. E.; Kolaczkowski, S. V.; Norris, J. R. In *Progress in Photosynthesis Research*; Biggins, J., Ed.; Martinus Nijhoff: Dordrecth, 1987; Vol. I.
(19) Haberkorn, R.; Michel-Beyerle, M. E. *Biophys. J.* **1979**, *26*, 489-498.
(20) Chidsey, C. E. D.; Takeff, L.; Goldstein, R. A.; Boxer, S. G. *Proc. Natl. Acad. Sci. U.S.A.* **1985**, *82*, 6850-6854.
(21) Gunner, M. R.; Robertson, D. E.; Dutton, P. L. *J. Phys. Chem.* **1986**, *90*, 3783-3795.

0002-7863/89/1511-3400$01.50/0

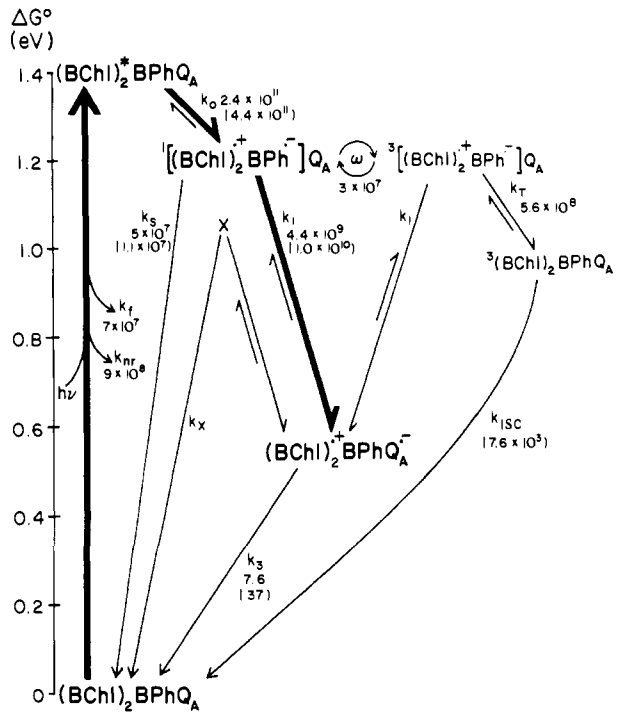

Figure 1. Electron-transfer pathways in the isolated RC. The forward, charge-separating reactions start with the absorption of a photon by a bacteriochlorophyll dimer $[(BChl)_2]$. This is promoted to the excited singlet state $(BChl)_2{}^*BPhQ_A$ [abbreviated as $(BChl)_2{}^*$ in the text]. Charge separation occurs at k_0,[12,13] yielding reduced bacteriopheophytin (BPh) and oxidized $(BChl)_2$, i.e., $(BChl)_2{}^{+\bullet}BPh^{-\bullet}Q_A$ [abbreviated $(BChl)_2{}^{+\bullet}BPh^{-\bullet}$]. $BPh^{\bullet-}$ then reduces a tightly bound ubiquinone-10 (Q_A) at k_1,[14] forming $(BChl)_2{}^{+\bullet}BPhQ_A{}^{-\bullet}$ [abbreviated $(BChl)_2{}^{+\bullet}Q_A{}^{-\bullet}$]. In vivo, cytochrome *c* reduces $(BChl)_2{}^{+\bullet}$ and Q_B, another bound ubiquinone, oxidizes $Q_A{}^{-\bullet}$. In the absence of donors or acceptors, electron transfer from $Q_A{}^{-\bullet}$ to $(BChl)_2{}^{+\bullet}$ returns the system to the ground state. This occurs either directly at k_3 or by a thermally accessible route via X.[15] The observed rate is referred to in the text as k_{back}. The relative free energy of X shown here assumes k_X is 7.7×10^{-7} s^{-1}. Several reactions compete with forward electron transfer. $(BChl)_2{}^*$ decays by fluorescence (at k_f)[16] or nonradiatively (at k_{nr}). $(BChl)_2{}^{+\bullet}BPh^{-\bullet}$ returns to the ground state by direct electron transfer at k_S.[17,18] Also, following spin rephasing to the triplet $^3[(BChl_2{}^{+\bullet}BPh^{-\bullet}]$,[19] charge recombination (at k_T) produces the triplet $(BChl)_2$ $[^3(BChl)_2]$.[20] $^3(BChl)_2$ relaxes either directly by intersystem crossing (at k_{ISC})[18-20] or by thermal repopulation of $^3[(BChl)_2{}^{+\bullet}BPh^{-\bullet}]$.[20] $^3[(BChl)_2{}^{+\bullet}BPh^{-\bullet}]$ may also decay directly to the ground state.[20] The effective rate of decay of $(BChl)_2{}^{+\bullet}BPh^{-\bullet}$ by all processes other than reduction of Q_A is referred to in the text as k_2. The electron-transfer rates are for the native RC, with UQ_{10} as Q_A, at room temperature. The rates in parentheses were determined below 100 K.

different free energies for the state $(BChl)_2{}^{+\bullet}Q_A{}^{\bullet-}$, which changes the $-\Delta G°$'s for the electron transfer from $BPh^{\bullet-}$ to Q_A as well as that from $Q_A{}^{\bullet-}$ to $(BChl)_2{}^{\bullet+}$.

The ability to vary the reaction $-\Delta G°$ as well as the temperature places this system in a unique position to explore electron-transfer theories as these are the observables that characterize the system in these theoretical models[32-37] (see ref 29-31 for reviews). However, prior to the work with Q_A-replaced RCs,[21] all studies, both in biological and in chemical systems, had been limited to changing either the temperature[14,22,38,39] or the $-\Delta G°$;[40-45] to our knowledge, no other electron-transfer reactions have been measured as a function of both parameters. Assumptions must be made in the analysis of experiments that monitor only one of these variables which may be shown to be unwarranted by a more complete study. For example, when the electron transfers in the native RC, summarized in Figure 1, were only studied as a function of temperature, the temperature independence of each was interpreted as resulting simply from the reorganization energy (λ) of the reaction being equal to its $-\Delta G°$.[30,31,46,47] This was an attractive possibility since all electron-transfer theories predict a reaction will be activationless when these two values are matched.[30,31,47] However, a reaction also will not show classical-Arrhenius behavior over a much more substantial free energy range if it is coupled to vibrations of energy ($\hbar\omega$) greater than or equal to the thermal energy at the temperatures explored in the experiment. It is not possible to distinguish between these two causes of temperature independence if the behavior of the reaction is known at only a single value for $-\Delta G°$.

Previous measurements with Q_A-replaced RCs characterized the direct electron transfer from $Q_A{}^{\bullet-}$ to $(BChl)_2{}^{\bullet+}$ as a function of both the $-\Delta G°$ and temperature.[21] The reaction rate (k_3) was found to be temperature independent from 5 to 200 K, over a $-\Delta G°$ range of approximately 800 meV rather than only in a limited region near $-\Delta G° = \lambda$. As the reaction was made more exothermic than in the native RC, the rate was only weakly dependent on the $-\Delta G°$. The analysis of this observation established that the vibrations coupled to the electron transfer included high-frequency, skeletal modes with $\hbar\omega \approx 200$ meV (1500 cm^{-1}). As the reaction was made less exothermic, the rate decreased, without becoming temperature dependent. It was shown that this could not be adequately explained if the reaction is coupled only to high-frequency modes plus vibrations of sufficiently small energy that they could be treated classically.

To further explore the behavior of the intra-RC reactions, especially in the region of small $-\Delta G°$, a study of the subnanosecond, charge-separating electron transfer from $BPh^{\bullet-}$ to Q_A was undertaken. This reaction has been well characterized in the native RC.[14,22,48-51] Changes in the rate (k_1) can be determined by measuring the quantum yield of $(BChl)_2{}^{\bullet+}Q_A{}^{\bullet-}$ (Φ_Q).[52] Φ_Q is at least 0.98 in the native RC at all temperatures.[53-55] The

(22) Schenck, C. C.; Parson, W. W.; Holten, D.; Windsor, W. W.; Sarai, A. *Biophys. J.* **1981**, *36*, 479-489.
(23) McElroy, J. D.; Mauzerall, D. C.; Feher, G. *Biochim. Biophys. Acta* **1974**, *333*, 261-277.
(24) Hales, B. J. *Biophys. J.* **1976**, *16*, 471-480.
(25) Cogdell, R. J.; Brune, D. C.; Clayton, R. K. *FEBS Lett.* **1974**, *45*, 344-347.
(26) Gunner, M. R.; Tiede, D. M.; Prince, R. C.; Dutton, P. L. In *Function of Quinones in Energy Conserving Systems*; Trumpower, B. L., Eds.; Academic Press: New York, 1982; pp 271-276.
(27) Kleinfeld, D.; Okamura, M. Y.; Feher, G. *Biophys. J.* **1985**, *48*, 849-852.
(28) Okamura, M. Y.; Isaacson, R. A.; Feher, G. *Proc. Natl. Acad. Sci. U.S.A.* **1975**, *72*, 3492-3496.
(29) DeVault, D. *Q. Rev. Biophys.* **1980**, *13*, 387-564.
(30) Jortner, J. *Biochim. Biophys. Acta* **1980**, *594*, 193-230.
(31) Marcus, R. A.; Sutin, N. *Biochim. Biophys. Acta* **1985**, *811*, 265-322.
(32) Ulstrup, J.; Jortner, J. *J. Chem. Phys.* **1975**, *63*, 4358-4368.
(33) Sarai, A. *Chem. Phys. Lett.* **1979**, *63*, 360-366.
(34) Kuznetsov, A. M.; Ulstrup, J. *Biochim. Biophys. Acta* **1981**, *636*, 50-57.
(35) Kakitani, T.; Kakitani, H. *Biochim. Biophys. Acta* **1981**, *635*, 498-514.
(36) Siders, P.; Marcus, R. A. *J. Am. Chem. Soc.* **1981**, *103*, 741-747.
(37) Siders, P.; Marcus, R. A. *J. Am. Chem. Soc.* **1981**, *103*, 748-752.
(38) DeVault, D.; Chance, B. *Biophys. J.* **1966**, *6*, 825-847.
(39) Peterson-Kennedy, S. E.; McGourty, J. L.; Hoffman, B. M. *J. Am. Chem. Soc.* **1984**, *106*, 5010-5012.
(40) Miller, J. R.; Beitz, J. V.; Huddleston, R. K. *J. Am. Chem. Soc.* **1984**, *106*, 5057-5068.
(41) Closs, G. L.; Calcaterra, L. T.; Green, N. J.; Penfield, K. W.; Miller, J. R. *J. Phys. Chem.* **1986**, *90*, 367-3683.
(42) Joran, A. D.; Leland, B. A.; Felker, P. M.; Zewail, A. H.; Hopfield, J. J.; Dervan, P. B. *Nature* **1987**, *327*, 508-511.
(43) Wasielewski, M. R.; Niemczyk, M. P.; Svec, W. A.; Pewitt, E. B. *J. Am. Chem. Soc.* **1985**, *107*, 1080-1082.
(44) McLendon, G.; Miller, J. R. *J. Am. Chem. Soc.* **1985**, *107*, 7811-7816.
(45) Closs, G. L.; Miller, J. R. *Science* **1988**, *240*, 440-447.
(46) Jortner, J. *J. Am. Chem. Soc.* **1980**, *102*, 6676-6685.
(47) Buhks, E.; Jortner, J. *FEBS Lett.* **1980**, *109*, 117-120.
(48) Kaufmann, K. J.; Dutton, P. L.; Netzel, T. L.; Leigh, J. S.; Rentzepis, P. M. *Science* **1975**, *188*, 1301-1304.
(49) Rockley, M. G.; Windsor, M. W.; Cogdell, R. J.; Parson, W. W. *Proc. Natl. Acad. Sci. U.S.A.* **1975**, *72*, 2251-2255.
(50) Peters, K.; Avouris, P.; & Rentzepis, P. M. *Biophys. J.* **1978**, *23*, 207-212.
(51) Pellin, M. J.; Wraight, C. A.; Kaufmann, K. J. *Biophys. J.* **1978**, *24*, 361-369.
(52) Kirmaier, C.; Holten, D.; Debus, R. J.; Feher, G.; Okamura, M. Y. *Proc. Natl. Acad. Sci. U.S.A.* **1986**, *83*, 6407-6411.

near-unity yield establishes that k_1 is much faster than the rates of other reactions available to $(BChl)_2^{\bullet+}BPh^{\bullet-}$. However, if the rate of forward electron transfer slows as the temperature or $-\Delta G°$ of the reaction is changed, Φ_Q will be reduced.

The direct measurement of Φ_Q as a function of $-\Delta G°$ can also address the requirements for the physiological function of the protein. The RC stores the energy of a photon as a disequilibrium in the redox energy of the system. However, in isolated RC, 860 meV of the 1380 meV of the absorbed photon is lost in the formation of $(BChl)_2^{\bullet+}Q_A^{\bullet-}$,[15,56] although this loss may be somewhat smaller in vivo if there is a membrane potential opposing charge separation. Monitoring the quantum yield of $(BChl)_2^{\bullet+}Q_A^{\bullet-}$ as the $-\Delta G°$ for forward electron transfer is diminished can determine how much of this large free energy drop is needed to maintain the high yield of charge-separated product.

Materials and Methods

RC was purified from *Rb. sphaeroides* bacteria strain R-26,[57] Q_A and Q_B were removed, and the protein was stored as described previously.[15,28]

Dr. J. Malcolm Bruce of the University of Manchester, U.K., kindly provided 2,7-dimethyl-9,10-anthraquinone and 2,7-dimethoxy-9,10-anthraquinone. 2-*tert*-Butyl-9,10-anthraquinone was purchased from Chemolog (South Plainfield, NJ). The sources of all other compounds were reported previously.[21] Quinone purity was established by HPLC.[58] Henceforth, the following abbreviations will be used: BQ, 1,4-benzoquinone; NQ, 1,4-naphthoquinone; 1,2-NQ, 1,2-naphthoquinone; AQ, 9,10-anthraquinone.

Sample Preparation. For room temperature, optical measurements, the samples contained 0.5–1 μM RC, 10 mM Tris-HCl, pH 8.0, 0.002% lauryldimethylamine oxide (LDAO), and 0.5–10 μM added quinone. For low-temperature, EPR studies, 20 μM RC, 10 mM Tris, 0.03% LDAO, 50% glycerol (v/v), and 40–150 μM added quinone was used. The data presented here were obtained with a single preparation of RC. Very similar results were found for each Q_A-replaced RC with at least one other preparation of protein.

Quinones dissolved in ethanol or dimethyl sulfoxide (DMSO) were added to the Q_A-removed RC diluted to the concentration used for measurement. For EPR measurements, sufficient quinone was added to saturate the Q_A binding site.[59,60] For optical studies, a mixture of Q_A-replaced RCs was prepared so that 40% of the RC contained UQ_{10} while 60% had the Q_A for which Φ_Q was to be determined. The concentration of ethanol or DMSO was less than 0.5% in the optical measurements and 4–10% in the samples for EPR. Room temperature controls established that as much as 10% ethanol or DMSO does not effect RC kinetics.

For optical studies at 295 K, the temperature of the curvette was controlled with a circulating water bath. For EPR measurements, the temperature was set and monitored as previously described.[21]

Characteristics of the Activating Flash. Reaction was initiated by a 10-μs (full width at half-maximum) xenon flash. For all EPR measurements, neutral density filters were used to attenuate the flash so that $\approx$40% of the RC absorb at least one photon.

For optical studies, the flash was masked with an IR-transmitting Kodak 88A wratten filter (cutoff at 700 nm). This excited 90% of the RC. The flash intensity was then varied with Kodak neutral density filters (0.1–2.5 N.D.). These are not "neutral" in the near-IR. A Beckman UV-visible-IR spectrophotometer measured the transmittance (Tr) at the two wavelengths for the protein's absorbance maxima in the near-IR. These values, weighted by the relative extinction coefficients of the absorbance bands,[61] were averaged to obtain the effective transmittance. The relative intensity of the flash (I') with each filter, which should be proportional to the number of photons absorbed by the RC, was defined as $(2 \times Tr_{804} + Tr_{865})/3$. I' with no neutral density filter is 1.0.

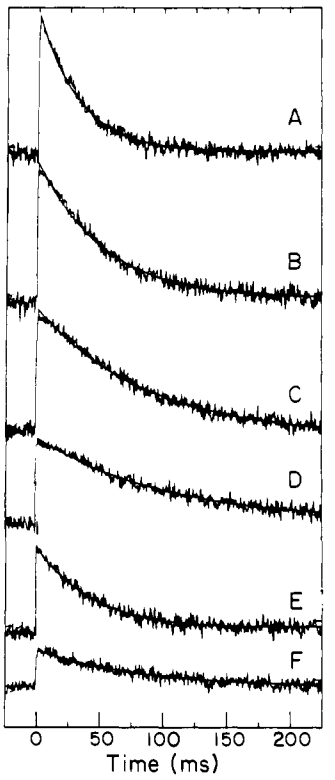

Figure 2. Flash-induced $(BChl)_2^{\bullet+}Q_A^{\bullet-}$ formation and decay monitored at the maximum of the first derivative of the $g = 2.0026$ EPR signal at 35 K. The samples all contained the same RC concentration (20 μM). The signal from the residual UQ_{10} found in all samples was subtracted from each trace by use of a theoretical transient with the same amplitude and kinetics as the signal found before quinone addition. A calculated transient was used for the background as this does not add additional noise to the signal. The theoretical lines represent at fit to one exponential plus a constant. The traces are for the following: (a) UQ_3, 30.5 s^{-1} with 0.5% constant; (b) 2,3-dimethyl-AQ, 18.7 s^{-1} with 1.6% constant; (c) 2-methyl-AQ, 11.4 s^{-1} with −3.3% constant; (d) 2-methoxy-AQ, 8.99 s^{-1} with −3.4% constant; (e) 2,3-dimethyl-AQ, 21.7 s^{-1} with −0.5% constant; (f) 2-amino-AQ, 11.8 s^{-1} with −1.4% constant.

Monitoring the $(BChl)_2^{\bullet+}Q_A^{\bullet-}$ Formed by the Flash. The concentration of RC in the state $(BChl)_2^{\bullet+}Q_A^{\bullet-}$ was determined from the oxidation state of $(BChl)_2$, measured by either dual-wavelength spectrophotometry at 602–540 nm[62] or by X-band EPR spectrometry at the maximum of the first derivative of the $(BChl)_2^{\bullet+}$ $g = 2.0026$ signal.[23] Both methods have been described previously.[21] For EPR, the microwave power was 15 μW at 14 K, 30 μW at 35 K, and 100 μW at 113 K. The $[(BChl)_2^{\bullet+}]$ with a lifetime greater than 30 μs was assumed to represent RC in the $(BChl)_2^{\bullet+}Q_A^{\bullet-}$ state (see Figure 1).

Determination of the Initial Concentration of $(BChl)_2^{\bullet+}Q_A^{\bullet-}$ Formed by the Flash. For the EPR measurements, the decay of the flash-induced kinetic transient, on a millisecond time scale, was fit to one exponential plus a constant[63] $[C_A \exp(-k_A t) + C_B]$ as described previously (see Figure 2).[21] The $[(BChl)_2^{\bullet+}Q_A^{\bullet-}]$ formed by the flash was taken to be the sum of the initial amplitudes of these components $(C_A + C_B)$. Controls with no added quinone established that the RC contained 10% residual UQ_{10}. This background signal was subtracted from the amplitude observed in the samples with added quinone.

For optical studies the native and Q_A-replaced RCs that were mixed together were distinguished by the rate of decay of $(BChl)_2^{\bullet+}Q_A^{\bullet-}$ (k_{back}) which is dependent on the $E_{1/2}$ of Q_A at room temperature (see Figure 3 and eq 5).[15,26] Φ_Q was not measured at 295 K when k_{back} for the particular quinone was between 3 and 15 s^{-1}, as these RCs could not be distiniguished from the population of RC containing UQ_{10}, where k_{back} is 7.6 s^{-1}, with sufficient certainty.

The decay of the kinetic transient from the mixture of RCs was fit by a linear least-squares analysis of the sum of two exponentials with known

(53) Wraight, C. A.; Clayton, R. K. *Biochim. Biophys. Acta* **1973**, *333*, 246–260.
(54) Loach, P. A.; Sekura, D. L. *Biochemistry* **1968**, *7*, 2642–2649.
(55) Cho, H. M.; Mancino, L. J.; Blankenship, R. E. *Biophys. J.* **1984**, *45*, 445–461.
(56) Arata, H.; Parson, W. W. *Biochim. Biophys. Acta* **1981**, *638*, 201–209.
(57) Clayton, R. K.; Wang, R. T. *Methods Enzymol.* **1971**, *23*, 696–704.
(58) Braun, B. S.; Benbow, U.; Lloyd-Williams, P.; Bruce, P. L.; Dutton, P. L. *Methods Enzymol.* **1986**, *125*, 696–704.
(59) Gunner, M. R.; Braun, B. S.; Bruce, J. M.; Dutton, P. L. (1985) in *Antennas and Reaction Centers of Photosynthetic Bacteria*; Michel-Beyerle, M. E., Ed.; Springer-Verlag: New York, 1985; pp 298–305.
(60) Gunner, M. R.; Braun, B. S.; Bruce, J. M.; Dutton, P. L., in preparation.
(61) Straley, S. C.; Parson, W. S.; Mauzerall, D. C.; Clayton, R. K. *Biochim. Biophys. Acta* **1973**, *305*, 597–609.
(62) Dutton, P. L.; Petty, K. M.; Bonner, H. S.; Morse, S. D. *Biochim. Biophys. Acta* **1975**, *387*, 536–556.
(63) Bacon, J. R.; Demas, J. M. *Anal. Chem.* **1983**, *55*, 653–656.

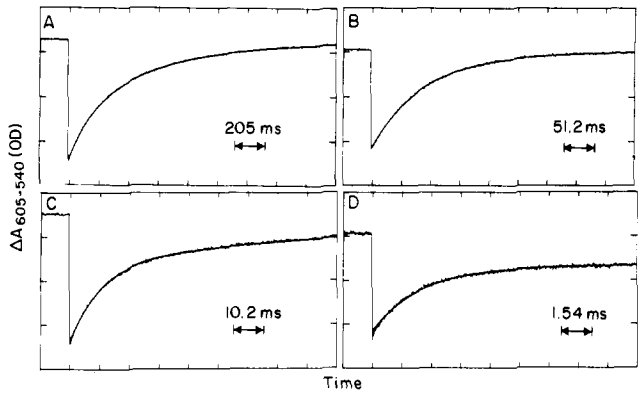

Figure 3. Flash-induced $(BChl)_2^{\bullet+}Q_A^{\bullet-}$ formation and decay at 295 K monitored at $\Delta A_{605-540}$ for Q_A-replaced RC mixed with native protein. The lines through the data represent a fit to two exponentials of known rate or two exponentials plus a constant. The vertical scale is $0.017\Delta A_{605-540}$ full scale. These samples were not matched for RC concentration. The traces are for the following: (a) tetramethyl-BQ, 66.4% at 1.8 s^{-1}, 31.2% at 7.6 s^{-1}, and 1.2% constant; (b) 2,3,5-trimethyl-BQ, 54.3% at 13 s^{-1}, 34.4% at 7.6 s^{-1}, and 1.2% constant; (c) AQ, 61.8% at 95 s^{-1} and 39.2% at 8.3 s^{-1}; (d) 1-methyl-AQ, 63.7% at 420 s^{-1} and 36.3% at 7.6 s^{-1}.

rate constants $[C_A \exp(-k_A t) + C_B \exp(-k_B t)]$. The values for k_{back} (k_A and k_B) were established in samples containing a homogeneous population of RC. The initial amplitude of each exponential provided the $[(BChl)_2^{\bullet+}Q_A^{\bullet-}]$ formed with each Q_A. When k_{back} values for the two quinones were of the same order of magnitude, the introduction of a constant significantly improved the fit. This slow component accounted for 1–3% of the total amplitude. Assigning this small portion of the total signal to either population of RC did not effect the results. When k_{back} for the experimental Q_A was approximately 10 times that of UQ, a slightly faster value for the UQ k_{back} improved the fit, suggesting some inhomogeneity in the lifetime with the native quinone as seen in the past.[23,64,65]

Theory for the Determination of Φ_Q from Light Saturation Measurements. Φ_Q was obtained from measurements of the $[(BChl)_2^{\bullet+}Q_A^{\bullet-}]$ as a function of the intensity of the activating flash. To obtain an analytic expression that describes how the $[(BChl)_2^{\bullet+}Q_A^{\bullet-}]$ formed by a flash depends on the electron-transfer kinetics, the reaction pathways in Figure 1 were simplified to Scheme I.

Scheme I

$$(BChl)_2BPhQ_A \underset{k_2}{\overset{kI'}{\rightleftharpoons}} (BChl)_2^{\bullet+}BPh^{\bullet-}Q_A \xrightarrow{k_1} (BChl)_2^{\bullet+}BPhQ_A^{\bullet-}$$

This assumes the following: (1) The rate of formation of $(BChl)_2^*$ is pseudo first order in light intensity with an effective rate constant of kI'. (2) The rate-determining step in $(BChl)_2^{\bullet+}BPh^{\bullet-}$ production is the absorption of a photon to form $(BChl)_2^*$. This holds under conditions where the rate of electron transfer from $(BChl)_2^*$ to BPh (k_0) is much faster than kI' and so is appropriate here, since the flash was barely saturating in 10 μs at maximum intensity ($kI' \leq 10^6$ s^{-1}) while $k_0 \geq 10^{11}$ s^{-1}. (3) The decay of $(BChl)_2^{\bullet+}BPh^{\bullet-}$ by all processes other than electron transfer to Q_A can be assigned a single rate constant (k_2). (4) The decay of $(BChl)_2^{\bullet+}BPh^{\bullet-}$ produces only $(BChl)_2^{\bullet+}Q_A^{\bullet-}$ or the ground state. (5) $(BChl)_2^{\bullet+}Q_A^{\bullet-}$ is stable during the lifetime of the flash.

The first two assumptions probably accurately describe the events in the RC, while the last three are approximations. Their effect on the analysis will be discussed below.

Given Scheme I, making a steady-state assumption for the concentration of $(BChl)_2^{\bullet+}BPh^{\bullet-}$ during the lifetime of the flash, the $[(BChl)_2^{\bullet+}Q_A^{\bullet-}]$ formed by the flash can be expressed as

$$[(BChl)_2^{\bullet+}Q_A^{\bullet-}] = [(BChl)_2^{\bullet+}Q_A^{\bullet-}]_{max}\left[1 - \exp\left(-\frac{k_1 kI'}{k_1 + kI' + k_2}t\right)\right] \quad (1)$$

where $[(BChl)_2^{\bullet+}Q_A^{\bullet-}]_{max}$ is the product formed with a fully saturating flash and t is the flash duration. A comparison of calculations using eq 1 with those employing the complete solution of the coupled differential equations solving Scheme I showed that the steady-state assumption is valid under conditions modeling these experiments.[66]

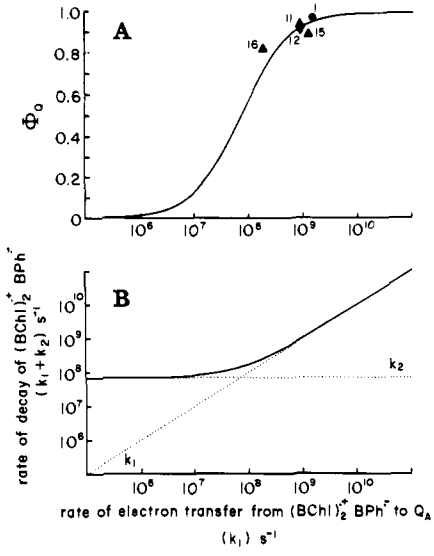

Figure 4. Comparison of the region of accuracy for the two methods for obtaining k_1. (A) Relationship between k_1 and Φ_Q calculated with eq 3. This method is seen to have its greatest sensitivity for $\Phi_Q < 0.9$. Although difficult to see in this figure, this method remains potentially useful at very low yields where Φ_Q is linearly dependent on k_1. The data points plot measured values for Φ_Q (Table I) against k_1 calculated from the rate of decay of $(BChl)_2^{\bullet+}BPh^{\bullet-}$ (ref 70). Numbers identifying the points refer to the first column of Table I. (B) Relationship between k_1 and the observed rate of decay of $(BChl)_2^{\bullet+}BPh^{\bullet-}$ occurring at $k_1 + k_2$. This method is most accurate when $k_1 > k_2$.

When $(k_1 + k_2) \gg kI'$, appropriate here, eq 1 further simplifies to eq 2, which was used to analyze the dependence of $[(BChl)_2^{\bullet+}Q_A^{\bullet-}]$ on the flash intensity and Φ_Q:

$$[(BChl)_2^{\bullet+}Q_A^{\bullet-}] = [(BChl)_2^{\bullet+}Q_A^{\bullet-}]_{max}(1 - \exp[-\Phi_Q(kI')t]) \quad (2)$$

where

$$\Phi_Q = k_1/(k_1 + k_2) \quad (3)$$

It is interesting to note that eq 3, the analytical expression derived from kinetic considerations of the system, is of the same form as the expression for the $[(BChl)_2^{\bullet+}Q_A^{\bullet-}]$ found after a flash derived by viewing excitation as a statistical process. The later assumes the number of photons absorbed by the RC during the flash can be described by a Poisson distribution (see ref 55 and 67 for extended discussion). Φ_Q now becomes the probability of forming product following excitation, while $kI't$ is the average number of photons absorbed per RC.

Calculation of k_1 from Φ_Q. Equation 3 defines Φ_Q as the outcome of a branching reaction which is implicit in Scheme I. It can be used to obtain k_1 from Φ_Q if k_2 is known. Schenck et al.[68] and Chidsey et al.[17] determined the rate of decay of $(BChl)_2^{\bullet+}BPh^{\bullet-}$ in RC where Q_A had been removed. They found that, despite the complexity of the reaction pathway, the decay could be described by a single exponential rate constant. This varied slightly with temperature and magnetic field. For the work presented here, k_2 will be taken to be 7.7×10^7 s^{-1} at 295 K, in the presence of zero applied magnetic field,[17,68] and 3.3×10^7 s^{-1} below 200 K, in the EPR spectrometer at a magnetic field strength of close to 3000 G.[17] Figure 4A shows the dependence of Φ_Q on k_1. The errors associated with the calculation of k_1 from Φ_Q have a very nonlinear dependence on the magnitude of this rate. When k_1 and k_2 are of the same order of magnitude, the yield should provide a sensitive measure of the electron-transfer rate. However, it should be noted that when the quantum yield is high ($\Phi_Q \geq 0.95$), Φ_Q provides only a lower limit for the rate ($k_1 \geq 20k_2$).

In addition, k_1 can be derived from the rate of decay of $(BChl)_2^{\bullet+}BPh^{\bullet-}$ which is assumed to occur at $k_1 + k_2$.[14,69,70] While this is the

(64) Kleinfeld, D.; Okamura, M. Y.; Feher, G. *Biochemistry* **1984**, *23*, 5780–5786.

(65) Loach, P. A.; Sekura, D. L. *Photochem. Photobiol.* **1967**, *6*, 381–393.

(66) Frost, A. A.; Pearson, R. G. *Kinetics and Mechanism: A Study of Homogeneous Chemical Reactions*, 2nd ed.; Wiley: New York, 1961; pp 173–177.

(67) Mauzerall, D. In *Biological Events Probed by Ultrafast Laser Spectroscopy*; Alfano, R. R., Ed.; Academic Press: New York, 1978; pp 215–235.

(68) Schenck, C. C.; Blankenship, R. E.; Parson, W. W. *Biochim. Biophys. Acta* **1982**, *680*, 44–59.

Table I. Temperature Dependence of Φ_Q

quinone	$E_{1/2}$ (meV)[a]	k_{back} (s^{-1})	Φ_Q 14 K[b]	Φ_Q 35 K[b]	Φ_Q 113 K[b]	Φ_Q 295 K[c]
1,4-benzoquinones						
(1) tetramethyl	30[e]	1.9	0.9 ± 0.07	0.92 ± 0.02	0.83 ± 0.05	0.97 ± 0.03
(2) UQ_3	0[f]	7.6	(1.00)[h]	(1.00)[h]	(1.00)[h]	(1.00)[h]
(3) decyl-UQ_0[d]	0[f]	3.3	0.88 ± 0.06	0.84 ± 0.04	0.81 ± 0.4	
1,2-naphthoquinone						
(4) unsubstituted	110[g]	2.1	0.44 ± 0.05	0.43 ± 0.03	0.37 ± 0.04	
1,4-naphthoquinones						
(5) unsubstituted	20[g]	8.0	0.72 ± 0.06	0.73 ± 0.05	0.66 ± 0.04	
(6) 2,3-dimethyl	−20[e]	8.8	1.01 ± 0.07	1.01 ± 0.06	0.96 ± 0.05	
(7) 2,3,5-trimethyl	−95[e]	12.7	1.01 ± 0.12	0.95 ± 0.05	0.86 ± 0.06	1.03 ± 0.05
(8) 5-methoxy	−115[e]	20.0	0.82 ± 0.07	0.80 ± 0.04	0.73 ± 0.06	0.91 ± 0.01
(9) 2-(dimethylamino)	−250	5400.0	0.35 ± 0.03	0.34 ± 0.04	0.29 ± 0.02	0.69 ± 0.05
9,10-anthraquinones						
(10) 1-chloro	−105	15.7	1.02 ± 0.07	0.98 ± 0.05	0.93 ± 0.08	0.96 ± 0.03
(11) 2-chloro	−110	17.8	0.69 ± 0.06	0.70 ± 0.03	0.60 ± 0.03	0.94 ± 0.01
(12) unsubstituted	−160	89.0	0.90 ± 0.10	0.90 ± 0.03	0.85 ± 0.07	0.92 ± 0.01
(13) 1-methyl	−200	425.0	0.78 ± 0.06	0.80 ± 0.05	0.64 ± 0.05	0.89 ± 0.01
(14) 1-methoxy	−235	1760.0	0.63 ± 0.05	0.69 ± 0.07	0.45 ± 0.06	0.81 ± 0.01
(15) 2-methyl	−245	2490.0	0.83 ± 0.05	0.85 ± 0.08	0.77 ± 0.07	0.90 ± 0.01
(16) 2-ethyl	−245	2270.0	0.53 ± 0.05	0.57 ± 0.03	0.43 ± 0.04	0.82 ± 0.01
(17) 2-*tert*-butyl	−255	3750.0	0.60 ± 0.05	0.55 ± 0.04	0.43 ± 0.02	0.78 ± 0.04
(18) 2-methoxy	−255	4050.0	0.67 ± 0.05	0.64 ± 0.04	0.41 ± 0.02	0.80 ± 0.01
(19) 1-amino	−270	7070.0	0.26 ± 0.03	0.26 ± 0.03	0.29 ± 0.02	0.64 ± 0.01
(20) 2,3-dimethyl	−290	13600.0	0.60 ± 0.08	0.60 ± 0.05	0.33 ± 0.02	
(21) 2,7-dimethoxy	−275[g]	>15000.0	0.15 ± 0.02	0.14 ± 0.03	0.05 ± 0.01	
(22) 2,7-dimethyl	−300[g]	>15000.0	0.49 ± 0.03	0.52 ± 0.06	0.20 ± 0.03	
(23) 2-amino	−420[g]	>15000.0	0.29 ± 0.02	0.25 ± 0.01	0.09 ± 0.01	

[a] $E_{1/2}$ for $Q_A/Q_A^{\bullet-}$ couple, relative to that found with UQ_{10} as Q_A. Unless otherwise noted, these were calculated with eq 5 from k_{back}. [b] Φ_Q calculated with eq 4 from $\Delta A_Q/\Delta A_{UQ}$ measured by EPR. The standard deviation represents the results of ΔA_Q determined twice for each of two samples. The uncertainty of ΔQ_{UQ} was included. [c] Φ_Q calculated with eq 2 from $\Delta A_{602-540}$ measured optically. The standard deviation is for three determinations of Φ_Q/Φ_{UQ}. [d] 2,3-Dimethoxy-5-methyl-6-decyl-1,4-benzoquinone. [e] Value from Woodbury et al.[15] [f] Assumed to be the same as when UQ_{10} is Q_A. [g] $E_{1/2}$ relative to UQ in Q_A site assumed to be the same as midpoint of $Q/Q^{\bullet-}$ relative to $UQ/UQ^{\bullet-}$ in DMF.[75] These values provide only an estimate of the in situ $E_{1/2}$. [h] Φ_{UQ} assumed to be 1.00. This provides a standard for all other determinations.

method of choice when $k_1 \gg k_2$, as k_1 slows the observed decay rate approaches k_2 and its sensitivity decreases. Figure 4 shows the range of rates for which each method is most accurate. The determination of k_1 for all Q_A-replaced RCs will require the use of both methods.

Measurement of Φ_Q. (A) Use of Native RC as a Standard for Determination of Φ_Q. The absolute quantum yield for RC with UQ_{10} as Q_A (Φ_{UQ}) has previously been measured to be 1.02 ± 0.04.[53-55] In addition, if the quantum yield of $(BChl)_2^{\bullet+}BPh^{\bullet-}$ is assumed to be 1.0, it can be calculated with eq 3. This yields a Φ_{UQ} of 0.984 at room temperature, zero magnetic field, and 0.997 below 200 K at 3000 G with measured values of k_1 (shown in Figure 1)[14] and k_2.[17,68] The existence of a standard with a known quantum yield allows Φ_Q to be determined with other Q_A's simply by comparing their yield relative to that found with native RC under the same conditions.

(B) Determination of Φ_Q at Room Temperature. For each sample, $[(BChl)_2^{\bullet+}Q_A^{\bullet-}]$ was measured at 16 different flash intensities (I'). $\Phi_Q kt$ was obtained from the best nonlinear least-squares fit to eq 2 calculated with the ASYSTANT software (McMillan Software Co., New York) for each of the two kinetically distinguishable RC populations in the sample. Since Φ_{UQ} was known, the ratio $(\Phi_Q kt)/(\Phi_{UQ} kt)$ for the two samples in the same curvette provided Φ_Q. Thus, the native RC provided an internal standard, which in an excellent control for any variation in the optical quality of different samples. A representative titration is shown in Figure 5.

(C) Determination of Φ_Q at Low Temperature. Φ_Q could not be determined at low temperature in the same manner as at 295 K. An internal standard cannot be used as readily, because at low temperature k_{back} for different Q_A-replaced RCs differs by less than a factor of 5.[21] In addition, as will be described below, the high yield of $^3(BChl)_2$ at low temperature[71] violates the assumptions made in deriving eq 2. Instead, Φ_Q was obtained from a comparison, at a single light intensity, of the amplitude of the $(BChl)_2^{\bullet+}$ signal in RC with the experimental Q_A (ΔA_Q) and that found with an identical concentration of protein reconstituted with UQ_3 (ΔA_{UQ}) with the relationship

$$\Delta A_Q/\Delta A_{UQ} = \Phi_Q/\Phi_{UQ} \quad (4)$$

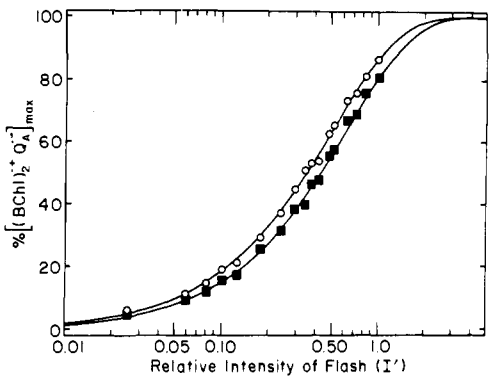

Figure 5. Light saturation curves for each component in a mixture of RC where 45% of the total [RC] have UQ_{10} as Q_A (○) and 65% have 2-ethyl-AQ (■). The theoretical line through the points represents the best fit to eq 2 of the initial concentration of $(BChl)_2^{\bullet+}Q_A^{\bullet-}$ for each kinetic component in the mixture as a function of relative intensity of the activating flash attenuated with a series of filters. The data are plotted for each Q_A as percent $[(BChl)_2^{\bullet+}Q_A^{\bullet-}]_{max}$ to show the difference in Φ_Q for the two quinones more clearly. Φ_Q for 2-ethyl-AQ is 0.82 if Φ_{UQ} is 1.00.

A comparison with eq 2 shows that eq 4 assumes the following:

(1) $kI't$ is the same for all samples. This requires that all samples have the same optical quality. While this is difficult to ensure in frozen glasses, variation in $kI't$ can be monitored by comparison of ΔA_Q for different samples with the same Q_A-replaced RC. The relative standard deviation of these measurements was generally ≤0.10 (see Table I).

(2) I' approaches zero so that each RC absorbs only one photon. Multiple excitations will cause eq 4 to provide too large a value for Φ_Q. However, at 40% light saturation, the conditions of the experiments reported here, the maximum error, near $\Phi_Q = 0.50$, is only 0.065. In addition, the high quantum yield for $^3(BChl)_2$ formation in RC that do not form $(BChl)_2^{\bullet+}Q_A^{\bullet-}$[71] reduces the error by diminishing the ability

(69) Liang, Y.; Nagus, D. K.; Hochstrasser, R. M.; Gunner, M. R.; Dutton, P. L. *Chem. Phys. Lett.* **1981**, *84*, 236-240.
(70) Gunner, M. R.; Liang, Y.; Nagus, D. K.; Hochstrasser, R. M.; Dutton, P. L. *Biophys. J.* **1982**, *37*, 226a.
(71) Wraight, C. A.; Leigh, J. S.; Dutton, P. L.; Clayton, R. K. *Biochim. Biophys. Acta* **1974**, *333*, 401-408.

Scheme II

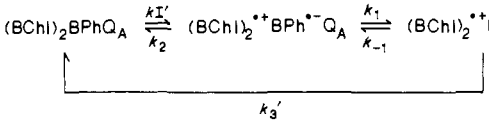

of multiple excitations to provide additional opportunities to generate $(BChl)_2^{\bullet+}Q_A^{\bullet-}$.

(3) $[(BChl)_2^{\bullet+}Q_A^{\bullet-}]_{max}$ is the same for all Q_A-replaced RCs. This requires that all RCs have a functionally bound Q_A. Dissociation constants (K_d) measured under somewhat different conditions (0.001% LDAO, 10 mM Tris-HCl, 0.5 μM RC) provide values of $\leq$0.1 μM for the AQ derivatives to 10 μM for NQ.[59,60] Thus, the quinone concentrations added should be more than adequate to saturate the Q_A site. In addition, Φ_Q is not correlated with K_d. In particular, the AQs, which generally have the smallest Φ_Q's, have very high affinities for the site.[60] Measurement of Φ_Q by complete light titrations does not require that the site be fully saturated, since eq 2 makes no assumptions about the value of $[(BChl)_2^{\bullet+}Q_A^{\bullet-}]_{max}$.

Validity of the Light Titration Method for Obtaining Φ_Q. Two of the assumptions about the reaction scheme made in the derivation of eq 1 do not apply under all conditions.

(1) Decay of $(BChl)_2^{\bullet+}Q_A^{\bullet-}$ during the Flash. It was assumed that $(BChl)_2^{\bullet+}Q^{\bullet-}$ is stable on the time scale of the flash; i.e., $1/k_{back} \gg$ flash duration ($\approx$10 μs). While this is true for all Q_A-replaced RCs below 200 K,[21] this is not the case at room temperature with low-potential Q_As (see Table I).

To explore the effects of the decay of $(BChl)_2^{\bullet+}Q_A^{\bullet-}$ during the flash on the value of Φ_Q obtained with eq 2, the reaction was modeled by Scheme II. The complete solution of the coupled differential equations was used to calculate $[(BChl)_2^{\bullet+}Q_A^{\bullet-}]$ at 10 μs for 15 values of kI' yielding 5–90% of $[(BChl)_2^{\bullet+}Q_A^{\bullet-}]_{max}$.[72] This provided a theoretical data set that simulated our experiments. Two pathways for the decay of $(BChl)_2^{\bullet+}Q_A^{\bullet-}$ were tested:

(a) The fast, thermal back-reaction repopulates $(BChl)_2^{\bullet+}BPh^{\bullet-}$ so that $k_{-1} = (k_{back}k_1)/k_2$ and $k_{3'} = 0$.

(b) Some other, unknown route is used so that $k_{3'} = k_{back}$ while $k_{-1} = 0$. When the results of these calculations were analyzed with eq 2, the values for Φ_Q and $[(BChl)_2^{\bullet+}Q_A^{\bullet-}]_{max}$ derived were smaller than the numbers initially assumed in the simulation. The error increased for larger values of k_{back}, and similar results were found with both models for the thermal decay of $(BChl)_2^{\bullet+}Q^{\bullet-}$. This is a consequence of the rapid decay of $(BChl)_2^{\bullet+}Q_A^{\bullet-}$ increasing the number of photons required to achieve a given $[(BChl)_2^{\bullet+}Q_A^{\bullet-}]$ at the end of the flash. However, for $k_{back} \leq 10^4$ s^{-1}, the limits of the measurements reported here, our simulations showed that fitting the data with eq 2 underestimates Φ_Q by less than 0.05. This was not considered to be a serious source of error, so this simple equation was used to fit the data from all light titrations.

(2) Alternate Decay Routes for $(BChl)_2^{\bullet+}BPh^{\bullet-}$. Scheme I and the equations derived from it assume that $(BChl)_2^{\bullet+}BPh^{\bullet-}$ forms only $(BChl)_2^{\bullet+}Q_A^{\bullet-}$ or the ground state. This ignores the production of $^3(BChl)_2$ which is formed in RC where Q_A has been removed or chemically reduced prior to the flash with a yield (Φ_T) of $\approx$0.3 at room temperature and $\geq$0.8 at low temperatures.[17,18,68,71,73] Preliminary calculations suggest that the formation of $^3(BChl)_2$ may cause the titrations to overestimate Φ_Q by a small amount. Unfortunately, Φ_T is not well established at room temperature. Estimates have ranged from 0.20[68] to 0.50.[74] Values of approximately 0.3 have been found under conditions similar to those of the work reported here.[17] However, because of this uncertainty, no corrections were made.

The $-\Delta G°$ for the Q_A-Involved Electron-Transfer Reactions. (A) The in Situ $E_{1/2}$ for $Q_A^{\bullet-}$. The $E_{1/2}$ values for $Q_A/Q_A^{\bullet-}$ were determined as described previously.[15,21] When the Q_A midpoint relative to that of the native RC was calculated from the rate of decay of $(BChl)_2^{\bullet+}Q_A^{\bullet-}$ via X (see Figure 1 and ref 15 for a discussion of X), the following relationship was used:

$$E_{1/2}(Q_A) - E_{1/2}(UQ) = -56.6 \times \log (k_{back} - 7.0) - 53.1 \text{ meV} \quad (5)$$

Measurement of the delayed fluorescence for a number of different Q_As, which is proportional to the $-\Delta G°$ between $(BChl)_2^*$ and $(BChl)_2^{\bullet+}Q_A^{\bullet-}$, was used to calibrate this line[15] (see ref 56 for a discussion of the method).

There are several Q_As for which there is no in situ $E_{1/2}$ value. An in vitro determination of the midpoint of the quinone (relative to UQ) in the aprotic solvent dimethylformamide provided an estimate for the midpoint of these Q_As (relative to UQ_A).[75] For Q_As where both in vitro and in situ measurements have been made, the former has been shown to be significantly less reliable.[15]

(B) $-\Delta G°$ for Electron Transfer from $BPh^{\bullet-}$ to Q_A. The $-\Delta G°$ for electron transfer from $BPh^{\bullet-}$ to Q_A with each Q_A was calculated from the $-\Delta G°$ for the reaction in the native protein and the replacement Q_A's $E_{1/2}$ relative to the value for UQ as Q_A. The midpoint of BPh was assumed to be independent of the identity of the quinone in the Q_A site.

There is some uncertainty about the magnitude of the $-\Delta G°$ between $(BChl)_2^{\bullet+}BPh^{\bullet-}$ and $(BChl)_2^{\bullet+}Q_A^{\bullet-}$ in the native RC. Values have been derived from several different kinds of experiments. Observation of delayed fluorescence by Parson and colleagues provides a value of 700 meV which decreases to 650 meV within approximately 10 ns.[76] At the lower limit, a $-\Delta G°$ of 510 meV is obtained from the measurement of k_{back} (on the microsecond to millisecond time scale) if X is assumed to be $(BChl)_2^{\bullet+}BPh^{\bullet-}$ (see ref 15 and 77 for a more complete discussion). More recently, Goldstein et al. have derived a value of 600 meV from determination of the free energy between $^3(BChl)_2$, $^3\{(BChl)_2^{\bullet+}BPh^{\bullet-}\}$, and the ground state (on the microsecond time scale).[78] For the present work a $-\Delta G°$ of 650 meV for the native RC has been assumed. This is from fluorescence measurements, which are made on a time scale closest to that of electron transfer from $BPh^{\bullet-}$ to Q_A. This uncertainty in the absolute reaction $-\Delta G°$ does not effect any of the qualitative conclusions that will be drawn here and has only limited consequences for the parameters that will be derived from the data.

Results

The quantum yield for $(BChl)_2^{\bullet+}Q_A^{\bullet-}$ production was measured for 16 different Q_A-replaced RCs at 295 K and for 22 different Q_As at 14, 35, and 113 K. The results are presented in Table I. By measuring the yield with a variety of quinone structures, it is possible to consider the variation of Φ_Q caused by modification of Q_A structure independently from that caused by changes in Q_A electrochemistry. This will provide an essential control for the theoretical analysis of the $-\Delta G°$ dependence of the rate.

Dependence of Φ_Q on Q_A Structure. The structure of the quinone reconstituting Q_A function was found to be relatively unimportant in determining the yield of $(BChl)_2^{\bullet+}Q_A^{\bullet-}$. Eight different Q_As (1 BQ, 3 NQs, and 4 AQs) were identified where Φ_Q was at least 0.9 at 295 K. At low temperature, the yield was at least 0.9 for RC with tetramethyl-BQ, 2,3-dimethyl-NQ, 2,3,5-trimethyl-NQ, and 1-Cl-AQ. With decyl-Q_0, 5-methoxy-NQ, and AQ it was at least 0.8.

The quinones that reconsitute high quantum yield for $(BChl)_2^{\bullet+}Q_A^{\bullet-}$ do not closely resemble UQ_{10}. Instead, they have a variety of structures and include compounds with one, two, and three rings substituted with methyl, decyl, methoxy, and chloro groups. With the exception of decyl-Q_0, with a 10-carbon, alkyl chain, none has a tail. Thus, the high quantum efficiency found in the native RC is not dependent on the structure of the native UQ_{10}. Of particular interest is that the long, 50-carbon, polyisoprenoid tail is clearly not required for this aspect of the quinone's function.

As shown by measurements with 1,2-NQ, not even the *p*-carbonyl structure of the native quinone is required to reconstitute Q_A function with significant quantum yield. However, this Q_A has a yield of only 0.4 ($\leq$113 K), suggesting that the *p*-carbonyl structure may be needed for Φ_Q to be close to 1.0.

$-\Delta G°$ Dependence of Φ_Q. The most striking result of the quantum yield measurements is the correlation of Φ_Q with the $E_{1/2}$ of Q_A (see Table I). This implies that the quantum yield is dependent on the $-\Delta G°$ of electron transfer from $BPh^{\bullet-}$ to Q_A. Figure 6 plots Φ_Q as a function of $-\Delta G°$ at 35 K. The pattern at all temperatures is as follows:

(72) Szabo, Z. G. In *Comprehensive Chemical Kinetics*; Bamford, C. H.; Tipper, C. F. H., Eds.; Elsevier, Amsterdam, 1969; pp 1–80.
(73) Boxer, S. G.; Chidsey, C. E. D.; Roelofs, M. G. *Annu. Rev. Phys. Chem.* **1983**, *34*, 389–417.
(74) Ogrodnik, A.; Krüger, H. W.; Orthuber, H.; Haberkorn, R.; Michel-Beyerle, M. E. *Biophys. J.* **1982**, *39*, 91–99.
(75) Prince, R. C.; Lloyd-Williams, P.; Bruce, J. M.; Dutton, P. L. *Methods Enzymol.* **1986**, *125*, 109–119.
(76) Woodbury, N. W. T.; Parson, W. W. *Biochim. Biophys. Acta* **1984**, *767*, 345–361.
(77) Shopes, R.; Wraight, C. A. *Biochim. Biophys. Acta* **1987**, *893*, 409–425.
(78) Goldstein, R. A.; Takiff, L.; Boxer, S. G., submitted for publication in *Biochim. Biophys. Acta*.

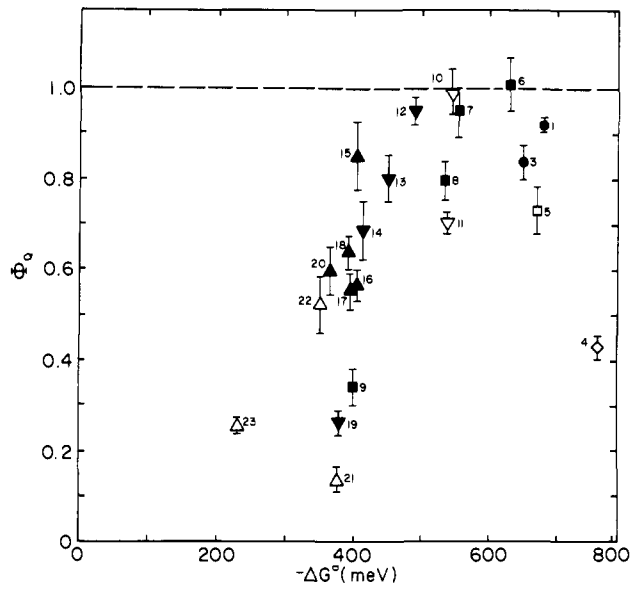

Figure 6. Quantum efficiency for formation of $(BChl)_2^{+\bullet}Q_A^{-\bullet}$ measured at 35 K as a function of the $-\Delta G°$ for the electron transfer from $BPh^{\bullet-}$ to Q_A. The data are taken from Table I. The quinones functioning as Q_A were (●) BQs, (□, ■) NQs, (◇) 1,2-NQ, (▽, ▼) AQ and 1-substituted AQs, and (△, ▲) 2-substituted AQs. The numerical labels refer to the first column in the table. Filled symbols imply the $-\Delta G°$ was calculated with Q_A $E_{1/2}$'s determined in situ while the open symbols use in vitro $E_{1/2}$ values. The $-\Delta G°$ in the native RC was assumed to be 650 meV.

(1) As the $-\Delta G°$ was decreased, relative to that found in the native RC, by as much as 150 meV or increased by at least 50 meV, Φ_Q remained relatively high (0.8–1.0) and apparently independent of $-\Delta G°$. This was found with RCs with 10 different Q_As.

(2) Once the $-\Delta G°$ was diminished by more than 150 meV, Φ_Q decreased as the reaction was made less exothermic. This was found with 12 different Q_As.

(3) There was a single Q_A where the $-\Delta G°$ had been increased by 110 meV which had a small yield. However, as it was the sole 1,2-quinone, this does not represent strong evidence for a general decrease in Φ_Q with increasing exothermicity. In addition, the $-\Delta G°$ for the reaction is not accurately known, as it was derived from in vitro $E_{1/2}$ measurements.

Calculation of k_1 from Φ_Q. The validity of calculating the rate of electron transfer from $BPh^{\bullet-}$ to Q_A from Φ_Q with eq 3 could be tested in a number of cases. For several Q_A-replaced RCs, k_1 had previously been obtained at 295 K from direct measurements of the rate of decay of $(BChl)_2^{\bullet+}BPh^{\bullet-}$ on the picosecond time scale.[69,70] This occurs at $k_1 + k_2$ and provides an accurate measure of k_1 when it is much faster than k_2 (see Figure 4B). The values obtained by these two methods were in good agreement (see Figures 4A and 7A).

Dependence of k_1 on $-\Delta G°$. The results of calculating k_1 from Φ_Q are shown in Figure 7. The pattern for the $-\Delta G°$ dependence of the rate is necessarily quite similar to that found for the yield. Thus, as the reaction was made less exothermic, there was initially little change in rate. This conclusion was reinforced by the picosecond measurements.[69,70] However, when the $-\Delta G°$ was decreased by more than 150 meV, k_1 became sensitive to the free energy, with the rate slowing as the reaction was made less exothermic. This pattern was repeated at all temperatures.

Temperature Dependence of Φ_Q and k_1. Data were obtained at 14, 35, and 113 K by the same method. However, measurements at 295 K were made by another technique. There are two issues that must be considered in comparing the results at room temperature and ≤113 K.

(1) While the light saturation technique for obtaining Φ_Q provides values with high reproducibility, their interpretation is unfortunately model dependent. Thus, as described under Materials and Methods, Φ_Q may be overestimated due to formation of $^3(BChl)_2$, while it may be underestimated when k_{back} is fast. Calculations of k_1 from Φ_Q presented here do not take this into account.

(2) k_2 at 295 K, zero magnetic field, is twice that found below 100 K at 3000 G.[17,68] Thus, the same rate of electron transfer from $BPh^{\bullet-}$ to Q_A will produce a smaller value for Φ_Q at room temperature. This is shown in the right vertical axis in Figure 8. This variation is included in the calculations of k_1 with eq 3.

The results of the measurement of Φ_Q at the four temperatures are shown in Figure 8. It was found that the determinations of 14 and 35 K provided very similar values for the yield, while slightly larger yields were obtained at 295 K.

An unexpected result is that the yield was significantly smaller at 113 K than at 14 or 35 K. A larger decrease was found in the range $0.2 < \Phi_Q < 0.8$, where Φ_Q is more sensitive to changes in k_1 (see Figure 4). Thus, it appears that the rate of electron transfer from $BPh^{\bullet-}$ to Q_A slows somewhat as the temperature is raised from 35 to 113 K and then becomes faster again as the system is warmed to 295 K. However, considering that these measurements cover a 20-fold change in thermal energy (from 14 to 295 K), it can be seen that with all Q_A-replaced RCs Φ_Q and k_1 are only weakly dependent on temperature.

Discussion

The measurements of the temperature and $-\Delta G°$ dependence of the rate of electron transfer from $BPh^{\bullet-}$ to Q_A allow this reaction to be analyzed by current electron transfer theories.[29-37] As these theories propose that vibrations in the redox sites and their surroundings are the source of the $-\Delta G°$ and temperature dependence of the rate, this should provide information about intra-RC nuclear motions involved in electron-transfer reactions.[29-37,79-85] The vibrations that are coupled to electron transfer are those for which the equilibrium bond length or frequency is different in reactants and products. Their frequency, ω, and the energy required for the changes, summarized as the reorganization energy (λ), connect theory to experimental observations.[29-33] To simplify calculations, most analyses, including the one used here, assume that there is no change in ω on reaction.[29-31,83]

A complete quantum mechanical description of the system provides the following expression for the rate with a single vibration coupled to the electron transfer:[29,32,36,37,84]

$$k = \frac{2\pi}{\hbar^2\omega}|V(r)|^2 e^{-S(2\bar{n}+1)}\left(\frac{\bar{n}+1}{\bar{n}}\right)^{P/2} I_P[2S\sqrt{\bar{n}(\bar{n}+1)}] \quad (6)$$

where $V(r)$ is the electron tunneling matrix element,[29,31,34] T is the absolute temperature, k_b is Boltzmann's constant, $\hbar\omega$ is the energy of the nuclear vibration coupled to electron transfer, S is $\lambda/\hbar\omega$, $\bar{n}$ is $[\exp(\hbar\omega/k_bT) - 1]^{-1}$, $I_p(z)$ is the modified Bessel function, and P is $-\Delta G°/\hbar\omega$ (see ref 29 and 84 for a detailed description of this equation). This expression calculates the thermally weighted contribution of the Franck–Condon overlap integral from each vibrational quantum level to the rate.

Dependence of the Expression Used To Calculate the Rate on the Energy of the Vibrations Coupled to the Electron Transfer. Equation 6 can be simplified in a manner that depends on the energy of the vibrations coupled to the electron transfer relative to the thermal energy of the system at the temperature of the experiment. Vibrations can be divided into three classes, designated small (S) where $\hbar\omega_S \ll k_bT$, intermediate (M) where $\hbar\omega_M \approx k_bT$, and large (L) for which $\hbar\omega_L \gg k_bT$. Each class contributes to the total reorganization energy of the system (λ_T) so that

$$\lambda_T = \lambda_S + \lambda_M + \lambda_L \quad (7)$$

(79) Warshel, A. *Proc. Natl. Acad. Sci. U.S.A.* **1980**, *77*, 3105–3109.
(80) Churg, A. K.; Weiss, R. M.; Warshel, A. *J. Phys. Chem.* **1983**, *87*, 1683–1694.
(81) Brunschwig, B. S.; Logan, J.; Newton, M. D.; Sutin, N. *J. Am. Chem. Soc.* **1980**, *102*, 5798–5809.
(82) Van Duyne, R. P.; Fischer, S. F. *Chem. Phys.* **1974**, *5*, 183–197.
(83) Marcus, R. A. *Annu. Rev. Phys. Chem.* **1964**, *15*, 155–196.
(84) Jortner, J. *J. Chem. Phys.* **1976**, *64*, 4860–4867.
(85) Bixon, M.; Jortner, J. *J. Phys. Chem.* **1986**, *90*, 3795–3800.

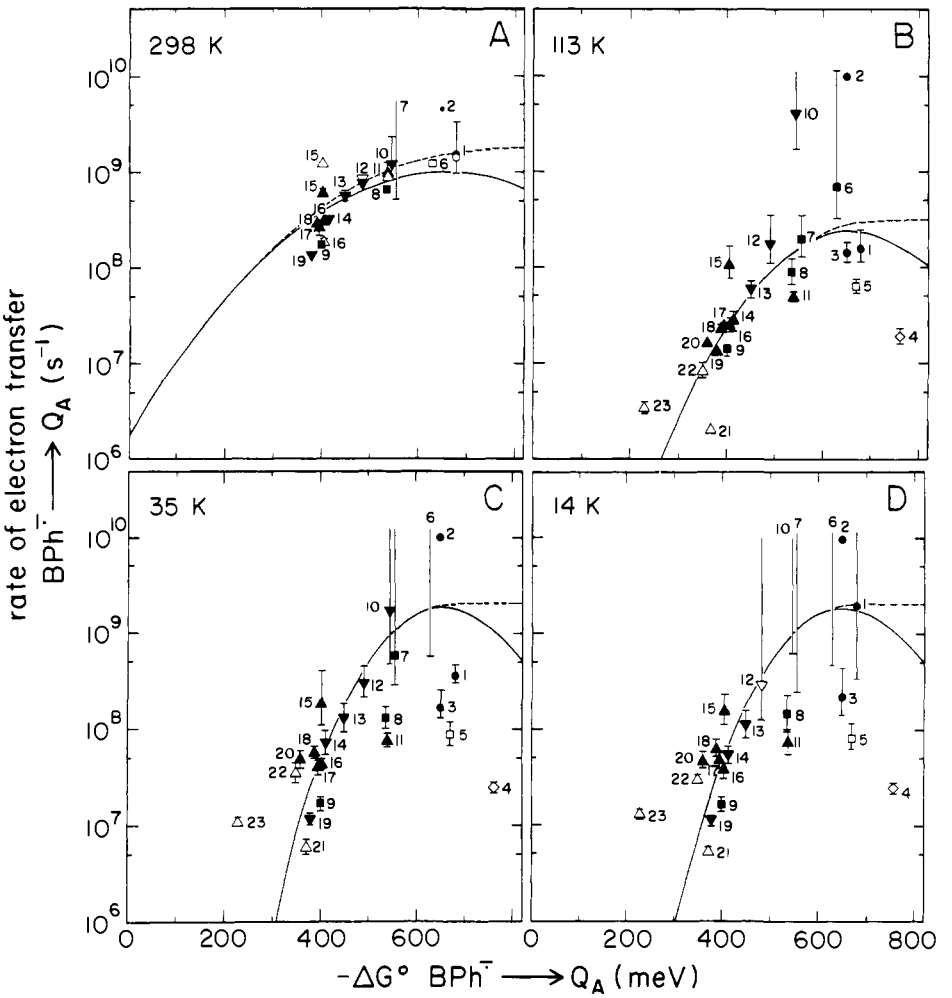

Figure 7. Dependence of k_1 on the $-\Delta G°$ for electron transfer from BPh$^{\bullet-}$ to Q_A measured at (A) 295, (B) 113, (C) 35, and (D) 14 K. The quinones are identified as in Figure 6 with the exception of panel A (295 K) where the open symbols represent values derived from picosecond measurements of the rate of decay of $(BChl)_2^{+\bullet}BPh^{-\bullet}$ at $k_1 + k_2$ (ref 70), filled symbols are for k_1 calculated from Φ_Q, and all $-\Delta G°$'s were calculated with Q_A $E_{1/2}$'s determined in situ. In all panels the rates were calculated from the values of Φ_Q listed in Table I with eq 3, corrected so that Φ_{UQ} is 0.984 at 295 K and 0.997 at all other temperatures. At 295 K, k_2 was assumed to be 7.7×10^7 s^{-1}; otherwise, a value of 3.3×10^7 s^{-1} was used. The error bars represent the variation in k_1 given the standard deviation of Φ_Q. If $\Phi_Q \geq 1.00$, k_1 is undefined. This is represented by error bars without fixed upper values when Φ_Q plus the standard deviation ≥ 1.0 and by error bars without data points when the average $\Phi_Q \geq 1.0$. The solid theoretical lines were calculated from eq 6 with $\hbar\omega_M = 15$ meV, $\lambda_M = 600$ meV, and $V(r) = 2.2 \times 10^{-1}$ meV at 295, 35, and 14 K and 8.7×10^{-2} meV at 113 K. The dashed lines were calculated with eq 11 with the same values with $\hbar\omega_L = 200$ meV and $\lambda_L = 200$ meV. At each temperature the value for k_1 for UQ_{10} (data point 2) was taken from ref 14.

Vibrations with small energy can be treated in the classical limit. For this to hold from 14 to 300 K, these should have an energy $\hbar\omega_S < 1$ meV (<8 cm^{-1}). The most widely used theory for electron transfer in chemical and biological systems considers only $\hbar\omega_S$, with λ_M and λ_L assumed to be zero, implying there are no changes in the large energy vibrations of the system on electron transfer. It connects the rate to the temperature and $-\Delta G°$ by the expression[29,31]

$$k = \frac{2\pi}{\hbar}\frac{|V(r)|^2}{\sqrt{4\pi\lambda_S k_b T}}\exp\left[-\frac{(\lambda_S - \Delta G°)^2}{4\lambda_S k_b T}\right] \quad (8)$$

This models the temperature independence of the electron transfer from BPh$^{\bullet-}$ to Q_A in the native RC, if that particular $-\Delta G°$ is assumed to equal λ_S.[30,31,46,47] It even accounts for the small observed increase in rate with decreasing temperature.[14,85] However, when $-\Delta G° \neq \lambda_S$, the reaction is predicted to have a classical, Arrhenius activation energy. The range of $-\Delta G°$ for which electron transfer from BPh$^{\bullet-}$ to Q_A and that from $Q_A^{\bullet-}$ to $(BChl)_2^{\bullet+}$ have been found to be temperature independent[21] shows that this simple theory, which treats nuclear motions in the classical limit, is inadequate for understanding electron transfer in RC at low temperature. Thus, electron transfer in RC is at most weakly coupled to small energy vibrations; otherwise, the reactions would slow dramatically with decreasing temperature as the $-\Delta G°$ was moved away from λ.

Calculations for the rates incorporating vibrations with intermediate energy (1 meV > $\hbar\omega_M$ > 100 meV) require use of eq 6 with no simplifications.

As vibrations with large energy ($\hbar\omega_L \geq 100$ meV) are defined as being frozen into their lowest level at all temperatures at which measurements are made, calculations need only consider that quantum state. Therefore, the expression for the rate given in eq 6 can be simplified to eq 9 which has no dependence on temperature,[29,36,46,47,84] where S' is $\lambda_L/\hbar\omega_L$ and P' is $-\Delta G°/\hbar\omega_L$.

$$k = \frac{2\pi}{\hbar^2\omega_L}|V(r)|^2\left(\frac{e^{-S'}S'^{P'}}{P'!}\right) \quad (9)$$

In addition, the rate can be calculated if the reaction is coupled to modes from more than one class of vibrations. If the reaction is coupled to small and high-energy vibrations, the rate will be given by[21,29,40,84]

$$k = \frac{2\pi}{\hbar}\frac{|V(r)|^2}{\sqrt{4\pi\lambda_S k_b T}}\sum_{q=0}^{\infty}\left(\frac{e^{-S'}S'^{q}}{q!}\exp\left[-\frac{(\lambda_S - \Delta G° - q\hbar\omega_L)^2}{4\lambda_s k_b T}\right]\right) \quad (10)$$

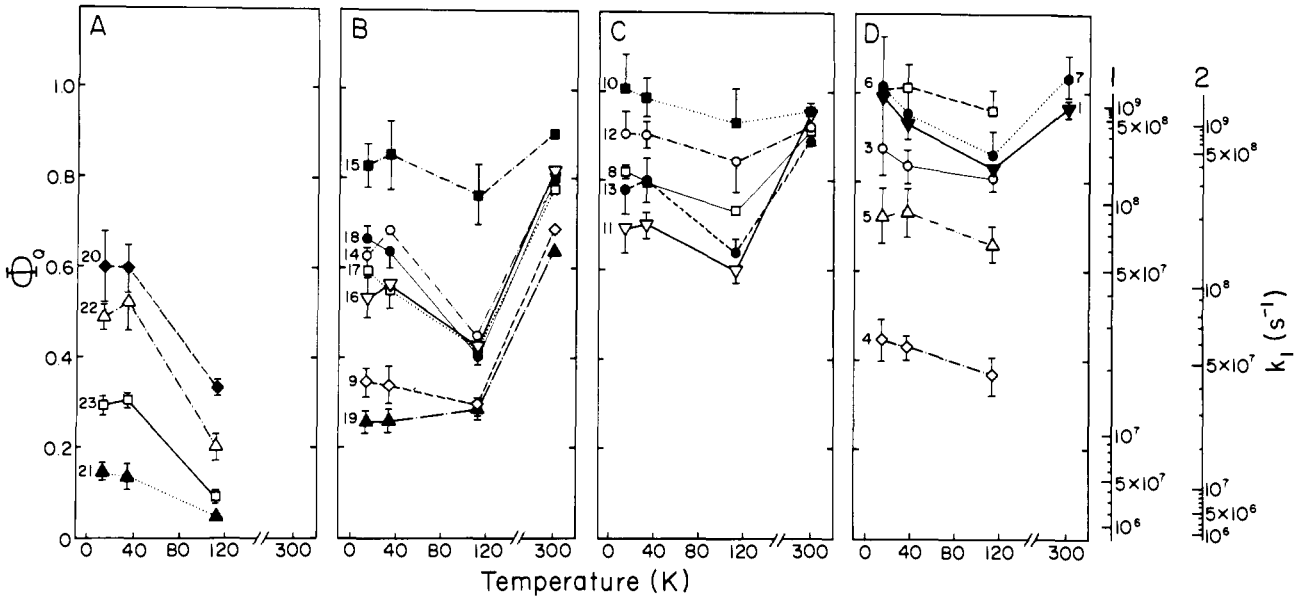

Figure 8. Φ_Q as a function of temperature. The data are from Table I. The numerical labels refer to the first column in the table. The $-\Delta G°$ for electron transfer from $BPh^{\bullet-}$ to Q_A was in the range (A) 230–375, (B) 380–415, (C) 450–545, and (D) 555–760 meV. The vertical axis on the right provides k_1 calculated with eq 3. (1) $k_2 = 3.3 \times 10^7$ s^{-1} (<200 K); (2) $k_2 = 7.7 \times 10^7$ s^{-1} (>200 K).

While if it is coupled to intermediate and high-energy vibrations, then

$$k = \frac{2\pi}{\hbar^2\omega_M}|V(r)|^2\sum_{q=0}^{\infty}\left(\frac{e^{-S'}S'^q}{q!}e^{-S(2\bar{n}+1)}\left(\frac{\bar{n}+1}{n}\right)^{P/2}I_P[2S\sqrt{\bar{n}(\bar{n}+1)}]\right) \quad (11)$$

where P is now $(-\Delta G° - q\hbar\omega_L)/\hbar\omega_M$.

A Distribution of Vibrations Is Required To Fit the Data. Equation 8 only defines the rate when $-\Delta G° = n\hbar\omega_M$ and eq 11 when $-\Delta G° = n\hbar\omega_M + q\hbar\omega_L$, where n and q are integers. However, the data show no quantum restrictions on allowed free energies. The lines drawn in Figures 7 and 9 simply ignore this, smoothly connecting the points calculated for the rate at the allowed $-\Delta G°$'s, an approximation that has been used previously (for example, see ref 85). Possible, more formal, solutions to the quantum limitations inherent in eq 8 and 11 include the following: (1) Addition of a distribution of medium-energy modes. This corresponds to providing these modes with a finite line width.[34] The values of $\hbar\omega_M$ and λ_M used here would therefore be representative, average values. (2) Calculation could include, in addition to medium- or high-energy vibrations, weak coupling to small-energy modes (e.g., eq 10); since they are treated in the classical limit ($\hbar\omega_S \rightarrow 0$), they provide a continuum of allowed $-\Delta G°$'s.[21] It should be noted that the magnitude of the vibrations has an effect on the value of $V(r)$ calculated from the observed rates. This can be seen by the inclusion of parameters dependent on the nuclei (for example, λ and ω) in the prefactors of eq 6–11.

Analysis of the Temperature and $-\Delta G°$ Dependence of the Rate of Electron Transfer. The electron transfer from $Q_A^{\bullet-}$ to $(BChl)_2^{\bullet+}$ (at k_3), another Q_A-involved intra-RC reaction, will be discussed along with the findings for k_1. This reaction rate was measured as a function of $-\Delta G°$ and temperature in an analogous study with Q_A-replaced RCs. The data, shown in Figure 9, are taken from ref 21. There are several advantages to considering both reactions together. The information about each reaction is more complete for a different range of $-\Delta G°$ values (relative to that of the native Q_A). There are more data for k_1 as the exothermicity is decreased, while the data set for k_3 provides more information in the region of increasing exothermicity. Also, the initial analysis of k_3 with eq 10 was only partially successful. It was shown that coupling to small and large modes could model the $-\Delta G°$ and temperature independence of the rate in the region of increasing free energy; however, it predicted strong temperature dependence when $-\Delta G° < \lambda_S$, which was not found. It will be shown here the results can in fact be well described by eq 11. In addition, the conclusions derived from the analysis of the two reactions can be compared to begin to identify general rules for electron-transfer reactions in RC.

Qualitative Analysis of the $-\Delta G°$ and Temperature Dependence of the Rate. Coupling of electron transfer to each class of vibrations provides a characteristic set of predictions for the temperature and $-\Delta G°$ dependence of the rate. In particular, each of the three classes is found to influence the rate most strongly in a different $-\Delta G°$ region. This allows a qualitative assessment of the data that provides a framework for a more quantitative analysis. Once modes of different energies are found to be coupled to electron transfer, a rough idea of their molecular character may be suggested by IR and Raman spectroscopy[86-88] as well as by calculations of the normal modes of proteins[80,86,89-91] and redox sites.[79,80]

(1) If the reaction is strongly coupled to small-energy vibrations when $-\Delta G° < \lambda_S$, the rate will decrease and will have significant classical, Arrhenius activation energy. Therefore, the lack of temperature dependence in each of the electron transfers studied demonstrates that λ_S is less than the smallest $-\Delta G°$ at which reaction has been measured.

(2) When the reaction is significantly coupled to intermediate-energy vibrations, the rate slows with decreasing exothermicity in the region $\lambda_S < -\Delta G° < \lambda_M$. However, little activation energy is expected as these vibrations, by definition, are only partially activated at the temperatures of the experiment. This is seen clearly for k_1 (at $-\Delta G° < 500$ meV) and with a smaller data set for k_3 (at $-\Delta G° < 400$ meV). The data for both reactions can be modeled if vibrations of $\approx$15 meV (120 cm^{-1}) are strongly coupled to electron transfer in RC.

(3) When the reaction is weakly coupled to high-energy vibrations [$0 < (\lambda_L/\hbar\omega_L) < 2$], the region of maximum rate beyond $-\Delta G° = \lambda_S + \lambda_M$ is broad, and although these reactions are still expected to experience exothermic rate restriction, the falloff in the rate with increasing exothermicity is quite gradual. This behavior is clearly seen in the $-\Delta G°$ dependence of k_3. The analysis of this reaction, either with eq 10 or with eq 11, suggests this electron transfer is coupled to vibrations of $\approx$200 meV (1500 cm^{-1}). There is as yet no data available for k_1 in this region of free energy.

(86) Krimm, S.; Bandekar *J. Protein Chem.* **1986**, *38*, 181–364.
(87) Tripathi, G. N. R. *J. Chem. Phys.* **1981**, *74*, 6004–6049.
(88) Clark, B. R.; Evans, D. H. *J. Electroanal. Chem.* **1976**, *69*, 181–194.

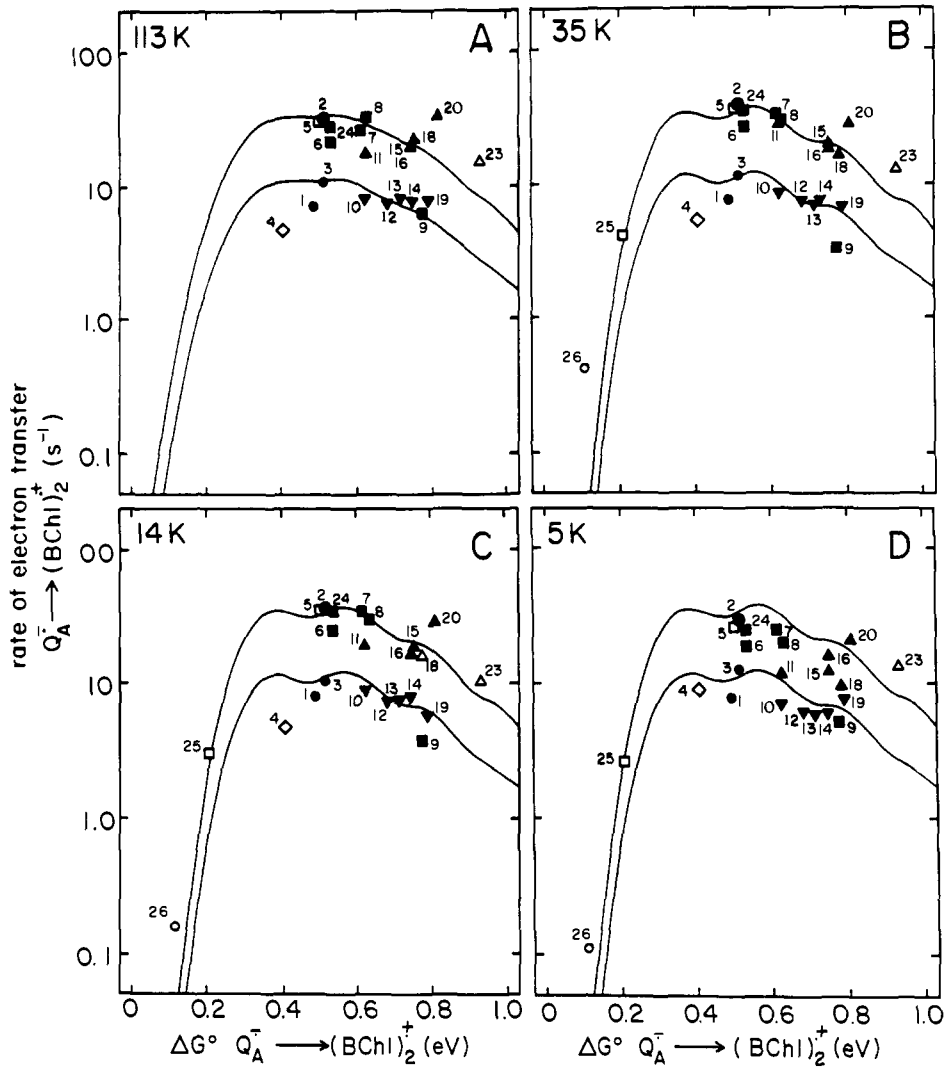

Figure 9. Rate of electron transfer from $Q_A^{\bullet-}$ to $(BChl)_2^{+\bullet}$, determined from the rate of decay of the flash-induced $(BChl)_2^{+\bullet}$ $g = 2.0026$ EPR signal as a function of the $-\Delta G°$ at (A) 113, (B) 35, (C) 14, and (D) 5 K. The data are from ref 21. The quinones are identified as in Figure 6. In addition, point 24 is for 2-methyl-3-prenyl-NQ as Q_A; point 25 is 2,3-dichloro-NQ; point 26 is 2,5-dichloro-3,6-dimethoxy-BQ. The $-\Delta G°$ with UQ as Q_A is 520 meV. The solid theoretical lines were calculated with eq 11 with $\hbar\omega_M = 15$ meV, $\lambda_M = 375$ meV, $\hbar\omega_L = 200$ meV, $\lambda_L = 200$ meV, and $V(r) = 2.6 \times 10^{-5}$ meV (upper curve) and 8.8×10^{-6} meV (lower curve).

With the multiparameter expressions used in calculating the rate, it is not possible to obtain exact numerical values for λ or $\hbar\omega$ in each class. Figures 7 and 9 provide one choice of values, and Figure 10 explores some of the limits that can be placed on them by the data. This shows that at low temperature it is possible to define $\hbar\omega_M$ within rather narrow limits. Better characterization of the rate at values of Φ_Q approaching 1.0 by picosecond measurements should allow an even better estimate. Also, it can be seen that at 295 K, where these vibrations are largely activated, no information can be derived about their magnitude. Thus, determination of the $-\Delta G°$ dependence of electron transfer when $\hbar\omega < k_bT$ is shown to provide information about the value of $\hbar\omega$ for the vibrations coupled to electron transfer.

Implications of Differences in $V(r)$, λ, or $\hbar\omega$ for the Different Q_A-Replaced RCs. (A) Q_A Dependence of $V(r)$. The observed rate is directly proportional to $|V(r)|^2$. An underestimate of the variation in $V(r)$ for the different Q_A-replaced RCs can cause the $-\Delta G°$ dependence of k_1 to be overestimated (e.g., see ref 85 and 21).

To determine how $V(r)$ changes with Q_A, data are needed in a free energy region where the rate is only weakly $-\Delta G°$ dependent. This is available for the electron transfer from $Q_A^{\bullet-}$ to $(BChl)_2^{\bullet+}$ (see Figure 9). Changes in Q_A bulk and geometry such as differences in the position of substitution on AQ, addition of tails to BQs, and the number of rings on the quinones appear to modify $V(r)$ by 2–5-fold. Thus, the dependence of $V(r)$ on the identity of Q_A is found to be relatively small, and it can be rationalized on the basis of the quinone structure. This establishes that if a sufficient number of replacements covering a large enough free energy range are studied, the $-\Delta G°$ dependence of this rate should not be obscured by variability in $V(r)$ (see 21 for a more complete discussion).

The study of k_1 provides little information on the exact dependence of $V(r)$ for that reaction on the structure of the replacement Q_A, because the most reliable determinations were in a region where $-\Delta G°$ strongly influences the rate. The picosecond studies do suggest that $V(r)$ may be approximately 3-fold smaller with the Q_A-replaced RCs than the value in the native protein (see Figure 7A).[69,70] The same factors that modify $V(r)$ for k_3 do not appear to correlate strongly with "scatter" in the plot of k_1 vs $-\Delta G°$ in Figure 7. More measurements of k_1, for Q_As where $-\Delta G° > 500$ meV, will be needed to resolve this issue. As these Q_As have high yield, this will require determination from the rate of decay of $(BChl)_2^{\bullet+}BPh^{\bullet-}$ rather than Φ_Q.

(B) Variation of λ or $\hbar\omega$ with Different Q_As. λ_T, its apportioning, and the energy of the different modes coupled to electron transfer may also be somewhat dependent on the structure of the different Q_As. However, it is likely that this variation will be correlated with different quinone structures (e.g., NQs vs AQs). In the work reported here there are enough quinone replacements that there are several Q_A-replaced RCs in each $-\Delta G°$ region. At the level of resolution of these measurements, there does not appear

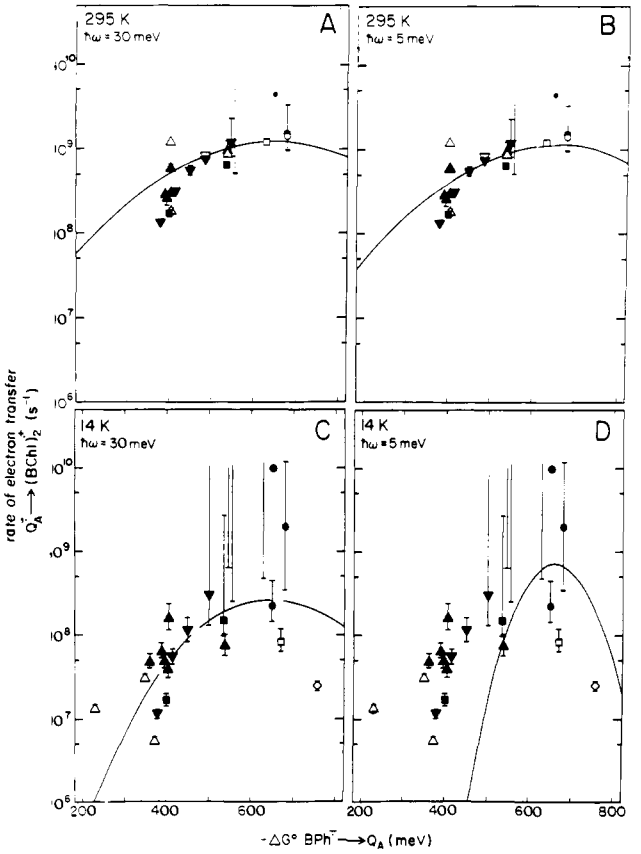

Figure 10. Alternate theoretical fits for the $-\Delta G°$ dependence of the rate of electron transfer from $BPh^{\bullet-}$ to Q_A at 295 K (A and B—the data are the same as found in Figure 7A) and 14 K (C and D—the data are identical with those in Figure 7D). The theoretical lines were calculated with eq 6 with λ_M = 660 meV and (A and C) $\hbar\omega_M$ = 30 meV and (B and D) $\hbar\omega_M$ = 5 meV.

to be any correlation of k_1 with the structure of the different Q_As.

(C) Details of the Temperature Dependence of k_1. Given that the reaction is coupled to vibrations where $\hbar\omega \approx k_bT$, it should be slightly temperature dependent over the range of temperatures covered. The activation energy should become greater as the $-\Delta G°$ is moved further from λ_M. In addition, since these vibrations are only beginning to be activated over the temperature region measured, the activation energy should increase as the temperature is raised. Thus given the fit parameters used in Figure 7 ($\hbar\omega_M$ = 15 meV, λ_M = 660 meV) at $-\Delta G°$ = 400 meV, there should be an increase in the rate of only 5% between 14 and 35 K, while the rate at 298 K should be 3 times as fast as that at 14 K. Thus, eq 8 or 11 models the general features of the dependence of k_1 on $-\Delta G°$ and temperature. This can be contrasted with the predictions of eq 8 (with λ_S = 660 meV and λ_M = 0), which predicts that, with a $-\Delta G°$ of 400 meV, the rate at 295 K should be 1800 times faster than that at 35 K and 6×10^8 times faster than that at 14 K. This is clearly not found.

However, eq 8 or 11 cannot accommodate the observation that k_1 is slower at 113 K than at the lower temperatures (see Figure 8). In the analysis used to calculate the theoretical lines plotted in Figure 7, the value used for $V(r)$ at 113 K was 2.25 times smaller than that at the other temperatures. This is a relatively small deviation from the predictions of theory. It may not be caused by a failure of theory but may instead represent temperature-dependent changes in the protein structure that can affect the tunneling pathway and so modify $V(r)$.[24,92] Similar problems were found in the analysis of a very detailed study of the temperature dependence of k_1 in the native RC by Kirmaier et al.[14] They suggested that changes in ω on electron transfer could account for the observations.[35]

(D) Temperature Dependence of the Reaction $-\Delta G°$. The possibility that $-\Delta G°$ varies with temperature could potentially affect the analysis. This is a general problem for studies covering such a large temperature range. There is some information about the temperature dependence of the energy levels of the redox states of the RC: The delayed fluorescence measurements suggest the energy of $(BChl)_2^{\bullet+}BPh^{\bullet-}$ increases as the temperature is lowered.[76] This would increase the $-\Delta G°$ for electron transfer from $BPh^{\bullet-}$ to Q_A if the free energy of $(BChl)_2^{\bullet+}Q_A^{\bullet-}$ is temperature independent. In contrast, analysis of the dependence of k_{back}[95] and triplet energies[78] on temperature provides a relatively constant value for the $-\Delta G°$ between $(BChl)_2^{\bullet+}BPh^{\bullet-}$ (or X) and $(BChl)_2^{\bullet+}Q_A^{\bullet-}$ and between $(BChl)_2^{\bullet+}$ and $^3(BChl)_2$, respectively. Additional work will be required to resolve this. At this time the $\Delta G°$ for the reaction with a given Q_A must be assumed to be the same at all temperatures. The assumption of ΔS = 0 is also made in the theoretical analysis when ω is assumed to be the same in reactants and products.[31]

Implications of the Temperature Independence of Electron Transfer in RCs. (A) Limits of Temperature Independence in RC Reactions. The majority of the intra-RC electron transfers are temperature independent, including the electron transfer from $(BChl)_2^*$ to BPh (k_0),[12] from $BPh^{\bullet-}$ to Q_A (k_1) (ref 14 and this work), from $Q_A^{\bullet-}$ to $(BChl)_2^{\bullet+}$(k_3),[21,23] and from $(BChl)_2^{\bullet+}BPh^{\bullet-}$ to the ground state (k_s)[70] (see Figure 1). This general observation had been proposed to imply that in the native RC the system is engineered so that $-\Delta G° = \lambda_T$ for each of these reactions.[30,31,46,47] The measurements reported here are consistent with $-\Delta G°$ for electron transfer from $BPh^{\bullet-}$ to Q_A and from $Q_A^{\bullet-}$ to $(BChl)_2^{\bullet+}$ being close to λ_T when UQ is Q_A (see Figures 7 and 9). However, the maintenance of temperature independence for k_1 and k_3 as the $-\Delta G°$ is changed shows that it is not possible to equate $-\Delta G°$ with λ_T simply because the reaction is not activated. Although this result might be obtained for fortuitous reasons, e.g., that λ_T is so dependent on Q_A in the modified-RCs that $-\Delta G°$ always equals λ_T, this is not necessary. A simpler and more attractive explanation is found by treating the vibrations coupled to electron transfer quantum mechanically. The observed behavior is explained simply by the reaction being primarily coupled to modes where $\hbar\omega \geq k_bT$. Thus, temperature independence arises because the nuclei as well as the electrons are quantum mechanical entities.

However, these theories do predict that the reactions should become temperature dependent if the $-\Delta G°$ or temperature is changed sufficiently. The regions of maximum sensitivity are as follows:

(1) If the electron transfers are coupled to intermediate-energy modes, they should become increasingly sensitive to temperature the further $-\Delta G°$ is from λ_M (see the theoretical lines in Figure 7). However, since by definition these modes are only partially activated at the temperatures of the experiments, the apparent activation energy should be small, and it should increase as the temperature is raised. Although for a reaction strongly coupled to a single vibration similar activation energy is expected at both decreasing and increasing $-\Delta G°$, it is more likely to be seen clearly at $-\Delta G° < \lambda_M$ because even weak coupling to high-energy vibrations will obscure the temperature dependence at increasing exothermicity.[32]

(2) If electron transfer is strongly coupled to small-energy modes, it should have an Arrhenius dependence on temperature when $-\Delta G° < \lambda_S$.

(89) Gō, N.; Noguti, T.; Nishikawa, T. *Proc. Natl. Acad. Sci. U.S.A.* **1983**, *80*, 3696–3700.
(90) Brooks, B.; Karplus, M. *Proc. Natl. Acad. Sci. U.S.A.* **1983**, *80*, 6571–6575.
(91) Jacrot, B.; Stephen, C.; Dianoux, A. J.; Engleman, D. M. *Nature* **1982**, *300*, 84–86.
(92) Feher, G.; Okamura, M. Y.; Kleinfeld, D. In *Protein Structure: Molecular and Electronic Reactivity*; Austin, R.; Buhks, E.; Chance, B.; DeVault, D.; Dutton, P. L.; Frauenfelder, H.; Gol'danskii, V. I., Eds.; Springer-Verlag: New York, 1987; pp 339–421.
(93) Debus, R. J.; Feher, G.; Okamura, M. Y. *Biochemistry* **1986**, *25*, 2276–2287.
(94) DeVault, D. *Photosynth. Res.* **1986**, *10*, 125–137.
(95) Gunner, M. R.; Dutton, P. L., unpublished observations.

Thus, the search for temperature dependence in RC should focus on reactions of small $-\Delta G°$. The current limit on the $-\Delta G°$ at which the reactions have been established to be temperature independent is 300 meV for the electron transfer from BPh$^{\bullet-}$ to Q_A (Figure 7), 150 meV from $Q_A^{\bullet-}$ to $(BChl)_2$ (Figure 9), and 250 ± 100 meV from $(BChl)_2$* to $(BChl)_2^{\bullet+}BPh^{\bullet-}$.[12] There are a number of reactions that do show activation energy which should be considered in order to reach a general conclusion about the magnitude of λ_S and λ_M in RCs.

(i) The electron transfer from cytochrome *c* to $(BChl)_2^{\bullet+}$ with a $-\Delta G°$ of 450 meV shows an activation energy of ≈200 meV.[29,38] This is still exciting theoretical analysis 20 years after the initial observation.[96,97] However, this electron transfer continues at cryogenic temperature only in RCs that have tightly associated *c* cytochromes. *Rb. sphaeroides* RCs do not fall in this class, and this reaction will not be considered further.

(ii) At room temperature, the decay to the ground state of $(BChl)_2^{\bullet+}Q^{\bullet-}$ with lower-potential Q_As is temperature dependent with an activation energy that is dependent on the Q_A $E_{1/2}$.[15,26,77] Also, the decay of $^3(BChl)_2$ has an E_a of 120 meV.[20] However, these are not considered to be direct, downhill reactions but rather to involve a higher energy intermediate. At low temperature both reactions occur at a temperature-independent rate that is assumed to represent the direct electron-transfer reaction.

(iii) The electron transfer from BPh$^{\bullet-}$ to $Q_A^{\bullet-}$ has been estimated to have a $-\Delta G°$ of ≈250 meV.[98] If this second reduction of Q_A is treated as being different from the first only because the $-\Delta G°$ is smaller, Figure 7 suggests that it should proceed with a rate of $\approx 9 \times 10^7$ s^{-1}, providing a Φ_Q of 0.54. Instead, this reaction occurs with negligibly low yield in the native RC. Okamura et al. measured a rate of 100 s^{-1} when UQ is Q_A, with an activation energy of 420 meV.[99] A part of this enormous difference in predicted and observed rates may be due to the actual $-\Delta G°$ being smaller than the current estimates, which are based on equilibrium measurements. These can provide time for proton binding or for motions of the protein or quinone that can stabilize the doubly reduced Q_A. However, the model used here predicts that the rate will be 1.7×10^6 s^{-1} even at $-\Delta G° = 0$. Thus to explain these results the analysis presented here may need to be modified to accommodate the data at smaller $-\Delta G°$ perhaps by considering some coupling to $\hbar\omega_S$. However, the observed rates may be a result of electron transfer to $Q_A^{\bullet-}$ being qualitatively different from reduction of Q_A for reasons that are as yet unknown or of the $E_{1/2}$ for $Q_A^{\bullet-}/Q_A^{2-}$ being lower than BPh/BPh$^{\bullet-}$ on the kinetic time scale so that the reaction is actually uphill.

(iv) The electron transfer from $Q_A^{\bullet-}$ to Q_B, the second bound ubiquinone in the native RC, has a $-\Delta G°$ of 90 meV and an activation energy of 590 meV.[100] However, RC can be prepared in a form so that this reaction becomes largely temperature independent.[64] Thus, temperature may control the rate by influencing a structural change within the protein or proton uptake, rather than the electron transfer. This reaction has the smallest $-\Delta G°$ of any of the intra-RC electron transfers.

Therefore, with the exception of cytochrome *c* oxidation, more work must be done to firmly establish whether any intra-RC electron transfer is temperature dependent. One implication of this observation is that electron transfer in RC protein is at most weakly coupled to vibrations of sufficiently small energy that they can be treated classically.

(B) Implications of λ_S Being Small. Vibrations coupled to electron transfer that can be treated classically have traditionally been identified with the motions in the material surrounding the electron donor and acceptor in response to electron transfer.[29,31,45,83,101,102] Determination of the $-\Delta G°$ dependence of the rate in chemical systems at room temperature[101,102] or at 77 K[41,42] has demonstrated that there is a substantial decrease in the reorganization energy of either small- or medium-energy modes when the dielectric constant of the solvent is diminished. A minimum value for this component of λ_T may be ≈150 meV found for electron transfer in isooctane.[41,45] These experiments have been modeled with eq 10, suggesting that λ_S is a measure of the solvent dielectric. However, measured at a single temperature, especially as warm as 77 K, the $-\Delta G°$ dependence of a reaction strongly coupled to $\hbar\omega_M$ or $\hbar\omega_S$, as defined here, is indistinguishable. Determination of the temperature dependence of these reactions, especially at lower temperatures, could make it possible to better characterize the energy of the vibrations whose reorganization energy changes as the solvent dielectric is varied. The solvents for these model systems are homogeneous solutions or disordered glasses which are quite different from the structured environment for electron transfer in proteins. Thus, the results of the measurements of temperature dependence in these systems may prove to be qualitatively different from those reported here.

It is clear that the Q_A-involved reactions in RC are only weakly coupled to vibrations that can still be treated in the classical limit down to 14 K, i.e., with energies <1 meV (<8 cm^{-1}). When these have been calculated for the normal modes of proteins,[88,89,90] they appear to generally represent motions involving large portions of the protein. Thus, the experiments reported here suggest that there is little coupling of electron transfer to large-scale motions of the protein.

(C) Importance of Intermediate-Energy Vibrations in the Electron-Transfer Reactions. The reactions are found to be strongly coupled to vibrations of ≈15 meV. In normal mode analysis of the proteins, it is suggested that modes of this energy may involve individual bonds[79,86] as well as vibrations of a few localized residues of the protein surrounding the redox sites.[86,89-91] Thus, it appears that only a small, local region of the protein responds to the change of oxidation state of a redox site. Vibrations of ≈12.5 meV (100 cm^{-1}) had been previously suggested to be coupled to electron transfer in RC.[85,92]

Another possible involvement of vibrations in this class has been proposed to rationalize the finding that Φ_Q is reduced to 0.47 and k_1 slows appropriately to 10^8 s^{-1} when the Fe^{2+} anti-ferromagnetically coupled to Q_A and Q_B is removed.[52,93] DeVault suggested that vibrations of the metal center are significantly coupled to the electron transfer, so that metal removal reduces the mass coupled to the reaction, thereby increasing λ_M.[94] If λ_T shifts enough so that it is now sufficiently larger than the $-\Delta G°$ in the native RC, the rate should slow. An alternative suggestion that iron removal decreases the $-\Delta G°$ of the reaction[52] is unlikely because of the insensitivity of k_{back}, which is considered to be an internal probe of this $-\Delta G°$,[15] to iron removal.

(D) Importance of Large-Energy Vibrations in the Electron-Transfer Reactions. It appears that the electron transfer from $Q_A^{\bullet-}$ to $(BChl)_2^{\bullet+}$ is weakly coupled to vibrations with $\hbar\omega_L \approx 200$ meV. Vibrations in this class have also been implicated in electron transfer in model systems.[40-42] Modes of this energy can generally be identified as being localized to a few atoms.[79,86] The importance of vibrations of this energy, such as carbon double bonds and carbonyl stretches, especially in electron transfer involving quinones, is not unexpected.[87,88] As can be seen in Figure 9, even weak coupling to high-frequency vibrations causes the electron transfer rate to fall off very slowly with increasing exothermicity. If this observation is general, then given the $-\Delta G°$ scale available to the RC, exothermic rate restriction cannot be used to favor the smaller $-\Delta G°$ energy conserving reactions over the more exothermic charge-recombining reactions.[30,31,46,47]

$-\Delta G°$ Dependence of k_1 and Φ_Q: Implications for RC Function. The function of the RC is to save the energy of the absorbed photon. If looked at solely in thermodynamic terms, the formation of $(BChl)_2^{\bullet+}Q_A^{\bullet-}$ proceeds with a substantial loss of free energy

(96) Bixon, M.; Jortner, J. *FEBS Lett.* **1986**, *200*, 303-308.
(97) Knapp, E. W.; Fischer, S. F. *J. Phys. Chem.* **1987**, *87*, 3880-3887.
(98) Rutherford, A. W.; Evans, M. C. W. *FEBS Lett.* **1980**, *110*, 257-261.
(99) Okamura, M. Y.; Isaacson, R. A.; Feher, G. *Biochim. Biophys. Acta* **1979**, *546*, 394-417.
(100) Mancino, L. J.; Dean, D. P.; Blankenship, R. E. *Biochim. Biophys. Acta* **1984**, *764*, 46-54.
(101) Brunschwig, B. S.; Creutz, C.; Macartney, D. H.; Sham, T. K.; Sutin, N. *Faraday Discuss. Chem. Soc.* **1982**, *74*, 113-127.
(102) Oevering, H.; Paddon-Row, M. N.; Heppener, M.; Oliver, A. M.; Cotsaris, E.; Verhoeven, J. W.; Hush, N. S. *J. Am. Chem. Soc.* **1987**, *109*, 3258-3269.

(see Figure 1). The experiments reported here show that much of this is required to maintain the high quantum yield. Thus, Φ_Q is found to decrease when $-\Delta G°$ for electron transfer from $BPh^{\bullet-}$ to Q_A is still greater than 300 meV, although the equilibrium constant at this point is more than 10^5 in favor of $(BChl)_2^{\bullet+}Q_A^{\bullet-}$ (see Figure 6). This occurs because of kinetic restrictions placed on the reaction by competing electron transfers. The maximum value for k_1 is only ≈50-fold faster than the rate of the competing reaction from $(BChl)_2^{\bullet+}BPh^{\bullet-}$. Therefore, to maintain a high quantum yield, $-\Delta G°$ must be close to λ_T, maintaining the fastest rate. Thus, energy conservation in the RC is found to be dominated by the relative kinetics of the competing reactions, rather than equilibrium constants for individual steps.

The electron transfer from $BPh^{\bullet-}$ to Q_A in *Rb. sphaeroides* RC may be compared with that found in *Rs. viridis*. In the latter protein the $-\Delta G°$ for electron transfer from $BPh^{\bullet-}$ to Q_A is 150 meV smaller than that in *Rb. sphaeroides* RC,[103] yet the quantum yield is ≈0.98 and k_1 is fast (4.3×10^9 s^{-1}).[104] Investigation of this rate with even a modest decrease in $-\Delta G°$ could establish if this protein exists closer to the edge of failure or if it has managed to reduce λ for the reaction.

The analysis of the reaction with current electron-transfer theories can provide a framework to consider the changes in the protein that could increase the free energy conserved in forming $(BChl)_2^{\bullet+}Q_A^{\bullet-}$. This could involve (1) decreasing $\lambda_S + \lambda_M$ to reduce the $-\Delta G°$ at which the rate is maximal, (2) increasing $V(r)$ by moving BPh and Q_A closer together, which would increase the rate at all $-\Delta G$'s, or (3) slowing k_2 in some manner so that k_1 could slow without Φ_Q diminishing.

(103) Prince, R. C.; Leigh, J. S.; Dutton, P. L. *Biochim. Biophys. Acta* **1976**, *440*, 622–636.
(104) Holten, D.; Windsor, M. W.; Parson, W. W.; Thornber, J. P. *Biochim. Biophys. Acta* **1978**, *501*, 112–126.

Conclusions

The analysis of the two Q_A-involved electron-transfer reactions in RC reported here shows that the pursuit of the $-\Delta G°$ dependence of electron transfer to low temperatures provides unique information about the nuclear motions coupled to an electron transfer. In particular, as the thermal energy drops significantly below $\hbar\omega$, reactions move out of the classical limit into a regime where the $-\Delta G°$ dependence of the rate becomes sensitive to the magnitude of $\hbar\omega$. Thus, these experiments provide estimates of the energy of the vibrations that are coupled to electron transfer which in turn suggest what aspects of protein and cofactor dynamics are important in the reaction. In addition, reactions are shown to be more sensitive to different parameters at different values of $-\Delta G°$ relative to λ or $\hbar\omega$. This aspect of the theory greatly simplifies the analysis, and it provides the basis for the general conclusions about the nature of the electron transfers in RC presented here.

Acknowledgment. We gratefully acknowledge John R. Miller and Joshua Jortner for the suggestion that the temperature and $-\Delta G°$ dependence of electron transfer in RC could be accounted for with the inclusion of quantized, low-frequency vibrations into the analysis. We thank Steve W. Meinhardt for technical assistance, Barry S. Braun for RC purification and quinone HPLC, Roger Prince for quinone electrochemistry, Malcolm Bruce and Ron Kaback for gifts of quinones, Chris Kirmaier and Dewey Holten for information concerning preliminary measurements of the rate of decay of $(BChl)_2^{\bullet+}BPh^{\bullet-}$ in Q_A-replaced RC, and Jean Wallace for very helpful discussion. This work was supported by NSF DBM 85-18433 and DOE-FG02-87-ER 10590.